2021-04-29

Efficacy of Connectivity-Based Targeting in TMS for Adolescents with Treatment-Resistant Depression

Tapia Palacio, Clara

UNIVERSITY OF CALGARY

Efficacy of Connectivity-Based Targeting in TMS for Adolescents with Treatment-Resistant Depression

by

Clara Tapia Palacio

A THESIS

SUBMITTED TO THE FACULTY OF GRADUATE STUDIES

IN PARTIAL FULFILMENT OF THE REQUIREMENTS FOR THE

DEGREE OF MASTER OF SCIENCE

GRADUATE PROGRAM IN NEUROSCIENCE

CALGARY, ALBERTA

APRIL, 2021

ABSTRACT

Background. Thirteen percent of 12- to 17-year-old adolescents suffer from depression, but only half respond to antidepressants and psychotherapy. Recent studies have successfully employed repetitive Transcranial Magnetic Stimulation (rTMS) to treat depression. However, there is a need to precisely determine the rTMS site of stimulation. A recent study in adults with depression (Fox et al., 2012) proposes that using the connectivity between the dorsolateral prefrontal cortex (DLPFC) and subgenual cingulate to define the site of stimulation for rTMS results in increased clinical efficacy. To date, no studies have investigated this phenomenon in the pediatric population.

Methodology. Functional magnetic resonance imaging (fMRI) scans of 37 adolescents with treatment-resistant depression (TRD) and 18 controls were analysed. TRD individuals underwent 15 consecutive rTMS sessions and were assessed for depression before and after treatment by the Hamilton Depression Rating Scale (Ham-D). We calculated the DLPFC-Subgenual connectivity for the seven different rTMS targeting approaches described in Fox et al. (2012). Then, we measured the DLPFC-Subgenual connectivity from the individual stimulation sites and explored any correlation with clinical efficacy.

Results. Contrary to Fox et al. (2012), four and three targeting approaches presented a positive correlation for the TRD and control groups respectively. Moreover, more positive values of DLPFC-Subgenual connectivity were significantly associated with a higher decrease in Ham-D scores (p = 0.025, one-tailed).

Limitations. We used coordinates for the targeting approaches and subgenual cingulate that had been originally defined in adults. Furthermore, small changes in the noise reduction procedure causes great divergence in the outcomes.

Conclusions. Since adolescents showed a distinctive and stronger functional connectivity between DLPFC and the subgenual cingulate, depression treatments have to be directly adjusted to pediatric population. Additionally, higher DLPFC-Subgenual positive connectivity predicted a higher clinical efficacy. This suggests that future work should consider defining the stimulation site at the DLPFC location with the strongest positive connectivity with the subgenual cingulate. However, the novelty of this research and the differences in outcomes with the literature in adult population indicates that reanalysing this association is necessary.

Keywords: Depression; resting-state functional MRI; adolescents; DLPFC; rTMS; DLPFC-Subgenual connectivity

PREFACE

This thesis is original, unpublished, independent work by the author, C. Tapia Palacio. The data analyzed in experiments one and two was previously collected in a registered clinical trial (ClinicalTrials.gov identifier NCT01731678). This trial was covered by Ethics Certificate ID 24656, first issued by the University of Calgary Conjoint Health Ethics Board on July 26, 2015.

ACKNOWLEDGEMENTS

I would like to express my deepest appreciation to my supervisor, Dr. Frank MacMaster. Without him, none of this would have even started. He trusted me to be part of his research group in the first place and has been there to help me throughout the entire process by providing excellent advice and guidance. Additionally, in this COVID era we are living in, he has always made my well-being and comfort the top priority and for that, I am forever thankful.

I would also like to extend my sincere gratitude to the other members of my Supervisory Committee: Dr. Katherine Rittenbach, Dr. Signe Bray and Dr. Daniel Kopala-Sibley. The numerous meetings we have had have been filled with many constructive suggestions, questions and discussions that in turn, have been the main source of growth and blossom of my thesis up to this final product.

I wish to thank the Alberta Children's Hospital Research Institute (ACHRI) for granting me the ACHRI Graduate Scholarship. Moreover, I want to acknowledge all the members of the ACHRI, as well as the Child and Adolescent Imaging Research (CAIR) trainees, administration, technicians and professionals, whose support has been essential for the successful development of the project.

I must also recognize my incredible lab peers, Dr. Sneha Chneji, Dr. Kayla Stone. Rose Swansburg, Tasmia Hai, Daria Merrikh and Allesha Eman. Their hard-work and passion to improve the lives of thousands of children with mental conditions has been so inspiring and has given much more meaning to the research I performed. They are all extremely bright women doing wonderful things. Furthermore, connecting with them on a weekly basis and sharing our respective research experience has smoothened the journey and has kept me grounded and sane. Among them, I want to send a special thanks to Dr. Sneha Chenji. She has been my go-to person at every step of the way. She has been next

to me through the good and not-so-good times, and I truly know it would not have been possible without her. It has been a teamwork at all times.

Last but not least, many thanks to the DINOS family. The women's basketball team of the University of Calgary are my family away from home. They have taught me so much about leadership and commitment, among million other values, and they are friends for life.

DEDICATION

To SARS-CoV-2…

Thank you for showing us how fragile mental health can be.

Thank you for reminding us to look after our loved ones.

Thank you for revaluing human connection.

Though you made it so hard, we accomplished it.

TABLE OF CONTENTS

LIST OF TABLES

LIST OF FIGURES

LIST OF SYMBOLS, ABBREVIATIONS AND NOMENCLATURE

MDD	Major Depressive Disorder
DSM	Diagnostic and Statistical Manual of Mental Disorders
ADHD	Attention-Deficit/Hyperactivity Disorder
MDE	Major Depression Episode
CBT	Cognitive Behavioural Therapy
CANMAT	Canadian Network for Mood and Anxiety Treatments
SSRI	Selective Serotonin Reuptake Inhibitor
TRD	Treatment-Resistant Depression
ATHF	Antidepressant Treatment History Form
TRSM	Thase and Rush Staging Model
TCA	Tricyclic Antidepressant
MAO	Monoamine Oxidase
MAOI	Monoamine Oxidase Inhibitor
ECT	Electroconvulsive Therapy
5-HT	5-Hydroxytryptamine
NE	Norepinephrine
DA	Dopamine
GABA	γ-Aminobutyric Acid
mPFC	Medial Prefrontal Cortex
IL	Interleukin
TNF-α	Tumor Necrosis Factor-α
BDNF	Brain-Derived Neurotrophic Factor
CRF	Corticotropin-Releasing Factor

MRI	Magnetic Resonance Imaging
fMRI	Functional Magnetic Resonance Imaging
fcMRI	Functional Connectivity Magnetic Resonance Imaging
DTI	Diffusion Tensor Imaging
PET	Positron Emission Tomography
EEG	Electroencephalography
VBM	Voxel-Based Morphometry
TMS	Transcranial Magnetic Stimulation
rTMS	Repetitive Transcranial Magnetic Stimulation
DBS	Deep Brain Stimulation
DLPFC	Dorsolateral Prefrontal Cortex
VLPFC	Ventrolateral Prefrontal Cortex
IC	Insular Cortex
dmPFC	Dorsomedial Prefrontal Cortex
NAc	Nucleus Accumbens
HF	High Frequency
LF	Low Frequency
FDA	Food and Drug Administration
AACAP	American Academy of Child and Adolescent Psychiatry
ACH	Alberta Children's Hospital
Ham-D	Hamilton Depression Rating Scale
FDI	First Dorsal Interosseous Muscle
LM1	Left Primary Motor Cortex
RM1	Right Primary Motor Cortex

BA	Broadmann Area
ACC	Anterior Cingulate Cortex
sgACC	Subgenual Anterior Cingulate Cortex
BOLD	Blood Oxygen Level-Dependent
DMN	Default-Mode Network
CEN	Central-Executive Network
FSL	FMRIB Software Library
TDC	Typically Developing Controls
K-SADS-PL	Kiddie Schedule for Affective Disorders and Schizophrenia Present and Lifetime
NDRI	Norepinephrine and Dopamine Reuptake Inhibitor
SNRI	Serotonin and Norepinephrine Reuptake Inhibitor
SARI	Serotonin Antagonist and Reuptake Inhibitor
GAD	Generalized Anxiety Disorder
PTSD	Post-Traumatic Stress Disorder
GE	General Electric
EPI	Echo-Planar Imaging
TR	Repetition Time
TE	Echo Time
FSPGR	Fast Spoiled Gradient Echo
BRAVO	Brain Volume
RMT	Resting Motor Threshold
MEP	Motor-Evoked Potentials
ROI	Region Of Interest
BET	Brain Extraction Tool

FEAT	FMRI Expert Analysis Tool
MCFLIRT	Motion Correction using FMRIB's Linear Image Registration Tool
FLIRT	FMRIB's Linear Image Registration Tool
FNIRT	FMRIB's Non-linear Image Registration Tool
MNI	Montreal Neurological Institute
FD	Framewise Displacement
EV	Explanatory Variable
ANOVA	Analysis Of Variance
ADAPT	Adolescent Depression and other Psychiatric Disorders

CHAPTER 1: INTRODUCTION

Basics of Major Depressive Disorder (MDD)

How is MDD defined?

Major Depressive Disorder (MDD) is characterized by the presence of sad, empty or irritable moods that substantially impact the individual's functioning in daily life. There are five criteria points for MDD to be diagnosed (see **Table 1**). Among the symptoms in the outlined criteria, either depressed mood (or irritable in children and adolescents) or diminished interest must be present. There are 14528 possible symptom combinations according to the DSM-IV and DSM-V criteria, illustrating the heterogeneity of MDD diagnosis (Zimmerman et al., 2014; Park et al., 2017). Each MDD diagnosis is defined based on whether it is a single or a recurrent episode, severity (mild, moderate, or severe), presence or absence of psychotic features, and remission status (partial or full). Neuroticism, adverse childhood experiences, stressful life events, having first-degree relatives with MDD, and the presence of substance use, anxiety or borderline personality disorders are recognized risk factors for MDD (American Psychiatric Association, 2013).

Table 1. Diagnostic Criteria for Major Depressive Disorder (MDD)

Diagnostic criteria for Major Depressive Disorder (MDD) in Diagnostic and Statistical Manual of Mental Disorders V (DSM-V). (American Psychiatric Association, 2013)

Criteria	Description
(A)	At least five of the following symptoms are constantly present during the same 2-week period (one of them must be either 1 or 2): 1. Depressed mood 2. Diminished interest or pleasure 3. Significant weight loss or weight gain, or decrease or increase in appetite 4. Insomnia or hypersomnia 5. Psychomotor agitation or retardation 6. Fatigue or loss of energy 7. Feelings of worthlessness or excessive guilt 8. Decreased ability to think, concentrate or make decisions 9. Recurrent thoughts of death
(B)	The symptoms cause clinical distress, or social or occupation impairment
(C)	The symptoms are not due to substance abuse or another medical condition
(D)	The episode is not explained by any schizophrenia spectrum or psychotic disorder
(E)	There has never been a maniac or a hypomanic episode

Does MDD differ in youth?

MDD presents differently in adolescents compared to adults. In youth, there is usually a greater variation in weight and appetite, less hypersomnia, fewer delusions, and decreased perception of psychomotor retardation and loss of energy (Mullen, 2018). Moreover, youth have a higher rate of recurrence and faster recovery of their depressive episodes. Unfortunately, depression in youth comes with serious consequences, including suicide, which is the second leading cause of death in adolescence (Centers for Disease Control and Prevention, 2021). Depression incidence increases suicide rate attempts from 3.3% to 22% in children and adolescents (Gould et al., 1998). More than half of adolescent victims of suicide have a depression disorder (Thapar et al., 2012), and data shows that 8% of adolescents with MDD will commit suicide by young adulthood (Mullen, 2018). Additionally, MDD throughout this period is related to substance misuse, obesity, and serious educational impairments (Thapar et al., 2012). It is common for adolescents with MDD to present conditions including attention-deficit/hyperactivity disorder (ADHD), anxiety disorder, disruptive disorder, substance use disorder, enuresis or encopresis, and/or separation anxiety disorder (Mullen, 2018). This bouquet of symptoms and diagnoses likely contributes to the high suicide rates observed in adolescent depression.

How common is MDD in youth?

Depression is a global public health issue. Currently, more than 300 million people suffer from depression, and this prevalence is increasing (Duda et al., 2020). In 2030, Major Depressive Disorder is expected to become the first cause of burden of disease worldwide (Malhi and Mann, 2018). In adulthood, MDD is as twice as frequent in women as in men (Kuehner, 2017).

The prevalence of MDD increases from early childhood through adolescence with rates of 0.5% in 3- to 5-year-olds, 6% in 6- to 11-year-olds, and 12% in 12- to 17-year-olds (Frieden et al., 2013; Mullen, 2018). According to the 2018 National Survey on Drug Use and Health, one in seven adolescents aged 12 to 17 had a Major Depression Episode (MDE) in the last year. Female teenagers appeared to be three times more likely to have experienced a recent MDE than males (Lipari and Park-Lee, 2019). This data suggests that the period of adolescence is uniquely vulnerable to depression. In fact, studies show that the window between 12 and 21 years old is a period with important changes in connections and myelination of the cortical and subcortical regions involved in emotion regulation, impulse control and executive functions (Lichenstein et al., 2016; Johnston et al., 2017; Croarkin et al., 2018; Lima-Ojeda et al., 2018). For this reason, mental health imbalances are common during adolescence, which leads to the onset of many psychiatric disorders, including depression (Tymofiyeva et al., 2020). Nonetheless, pediatric depression is often underdiagnosed, and less than half of the cases of youth depression receive treatment before the age of 18 (Kessler et al., 2001; Mullen, 2018).

Treatments for MDD in Youth

Treatment for adolescents with MDD combines psychoeducation, individual psychotherapy, family interventions and pharmacotherapy (Croarkin and MacMaster, 2019). For mild cases, psychoeducation and psychotherapy are effective in 62% of patients (Mullen, 2018). Education generally consists of informative sessions involving close relatives so that they become "informed partners" in the recovery process. The most common form of individual therapy is cognitive behavioural therapy (CBT), which has the objective of addressing cognitive biases

that may trigger and maintain depressive behavior and thoughts (Park and Goodyer, 2000). According to the Canadian Network for Mood and Anxiety Treatments (CANMAT) guidelines, antidepressants, in combination with psychotherapy, are the first-line treatment for moderate-to-severe depression. Selective serotonin reuptake inhibitors (SSRIs) are the most used medication for MDD in youth (MacQueen et al., 2016). SSRIs improve symptoms of depression by reducing the synaptic reuptake of serotonin, which increases the availability of serotonin in the synaptic cleft (Chesebro et al., 2019). Fluoxetine is a first-choice SSRI, followed by escitalopram and sertraline, which are considered second-choice medications because these medications have shown smaller effects with respect to placebo, and there are fewer pieces of evidence in the literature to support their efficacy compared to fluoxetine. The CANMAT guidelines advise to trial antidepressants for 6-12 months in patients without previous depressive episodes, and for at least one year for adolescents with two or more MDE, or one severe or chronic episode (MacQueen et al., 2016). These mentioned recommendations are based on adult MDD research as studies regarding pediatric MDD pharmacology are rather limited.

How is Treatment-Resistant Depression (TRD) defined in research and practice?

Despite the extensive use of psychotherapy and medication to treat depression, 40% of total patients with MDD are resistant to these treatments (Lefaucheur et al., 2020). There is no universal definition for TRD, and a lack of consensus between researchers and clinical professionals. In a systematic review conducted by Brown et al. (2019), 155 different definitions were found in 150 articles. In those, the most common approaches to define TRD were the staging models such as the Antidepressant Treatment History Form (ATHF) and the Thase and Rush Staging Model (TRSM), or the treatment failure method, in which the TRD is determined

based on a certain amount of failed psychotherapy or pharmacology rounds. 50.3% of the definitions included a minimum of two unsuccessful treatment trials (Brown et al., 2019; Voineskos et al., 2020). In clinical practice, the term TRD is rarely used. Instead, physicians tend to refer to those cases with the following concepts: “recurrent or relapsing depression,” “complex depression,” “difficult to treat,” “multiple episodes of depression,” “chronic depression,” and “struggled with depression throughout their lives” (Brown et al., 2019).

The risk for relapse and chronification is 85% and 20% respectively in adult MDD (Lefaucheur et al., 2020). In children and adolescents, the rates of antidepressant response and remission are even lower (Chen et al., 2020; MacMaster et al., 2019), with almost 50% of pediatric depression cases reported as TRD (Lefaucheur et al., 2020; MacQueen et al., 2016). Once a patient has failed to the first round of antidepressants, treatment guidelines suggest trying another pharmaceutical option (e.g. other SSRI, TCAs, or MAOIs), or a neurostimulation technique such as transcranial magnetic stimulation (TMS) or electroconvulsive therapy (ECT). ECT is only recommended for very severe episodes of depression, such as MDD with psychotic features (Lefaucheur et al., 2020; MacQueen et al., 2016). Although neurostimulation is showing encouraging results, to treat TRD, there are some pieces missing. A target derived from an understanding of the underlying pathophysiology of the disorder is lacking at present.

What do we know about the pathophysiology of MDD?

In spite of the numerous research studies conducted regarding the basis of depression, the pathophysiology of MDD is still not fully understood. MDD is considered a complex disease with many possible causal mechanisms, and not all of these mechanisms are necessary to

present MDD. For many years, the monoamine hypothesis of depression dominated the field, which states that the depletion of serotonin (5-HT), norepinephrine (NE), dopamine (DA) and/or monoamine oxidase enzymes (MAO) in neuronal synapses leads to alterations in mood in MDD patients. Although being overly simplistic, this hypothesis resulted in the development of antidepressants (Dean and Keshavan, 2017). Other studies have shown that glutamate and γ-aminobutyric acid (GABA) are decreased in depression in regions such as the medial prefrontal cortex (mPFC) and the amygdala. More recent evidence has established the neuroimmune hypothesis, which attributes altered neurobiological structure and function in MDD to a chronic overstimulation of immune cells including microglia, monocytes and macrophages. Several cytokines such as interleukin-1 (IL-1), interleukin-6 (IL-6) and tumor necrosis factor-α (TNF-α) are overexpressed in patients diagnosed with depression. Brain-derived neurotrophic factor (BDNF), a neurotrophin that promotes survival of existing neurons, and growth and differentiation of new neurons, is reduced in depression as well. This suggests that neurogenesis and neuroplasticity are affected in MDD. Finally, a dysregulation of the HPA axis and a hyperactive response to stress has been associated with MDD. Particularly, patients with depression have shown excessive secretion of corticotropin-releasing factor (CRF), impaired negative feedback, increased size of adrenal glands, hypercortisolemia and enlarged pituitary gland (Dean and Keshavan, 2017; MacMaster et al., 2006; Pitsillou et al., 2020).

From a systematic perspective, the limbic system and the cortical cognitive networks are dysregulated in depression (Pitsillou et al., 2020). These systems are reciprocally interconnected and work collectively in emotion regulation. Neuroimaging techniques [i.e. functional magnetic resonance imaging (fMRI) to evaluate brain activity, diffusion tensor imaging (DTI) for white matter integrity (Smith and Jakobsen, 2013), positron emission tomography (PET) to study the

dynamics of molecular processes in the brain, electroencephalography (EEG) for brain activity with high temporal resolution, and voxel-based morphometry (VBM) to identify local neuroanatomical differences] together with neurostimulation procedures [i.e. repetitive transcranial magnetic brain stimulation (rTMS), deep brain stimulation (DBS), and optogenetics] have been essential to identify the circuitry abnormalities in MDD, although there is a lack of consistency (Park et al., 2019). Patients with depression show (1) hyperactivity of the amygdala with response to negative stimuli; (2) increase in mPFC activity and resting-state subgenual cingulate and thalamic functional connectivity, which are regions involved in rumination and self-referential thoughts; (3) decreased left dorsolateral prefrontal cortex (DLPFC) activity, and hyperactivity of the right DLPFC, which is coherent with the symptoms of excessive anticipatory anxiety and difficulty disengaging from aversive input found in depression; (4) heightened attention to environmental negative stimuli due to hypoactivity of the ventrolateral prefrontal cortex (VLPFC); (5) impaired functioning and decreased volume of the dorsomedial prefrontal cortex (dmPFC), associated with difficulties in separating the emotional states from salient thoughts; and (6) reduction of the volumes of the nucleus accumbens (NAc, involved in reward and motivation) and the subgenual cingulate by up to 48% (Park et al., 2019; Pizzagalli et al., 2009; Sheline, 2003). **Figure 1** summarizes the activity differences between healthy and MDD individuals in the regions involved in emotion regulation. As can be perceived, the abnormalities in the affect regulation system are very diverse, and the relationships between these systems and cellular and molecular irregularities is unclear. Recent efforts have been dedicated to developing a unified theory of depression, including all the fundamental mechanisms, circuit abnormalities, and how they interconnect (Dean and Keshavan, 2017; Pitsillou et al., 2020). However, having that many representations of

depression, it could be questioned whether or not they all have the same origin. In any case, only a deeper understanding of the changes in depression at the molecular level can lead us to unravel the relationships between the possible abnormalities presented in this disease.

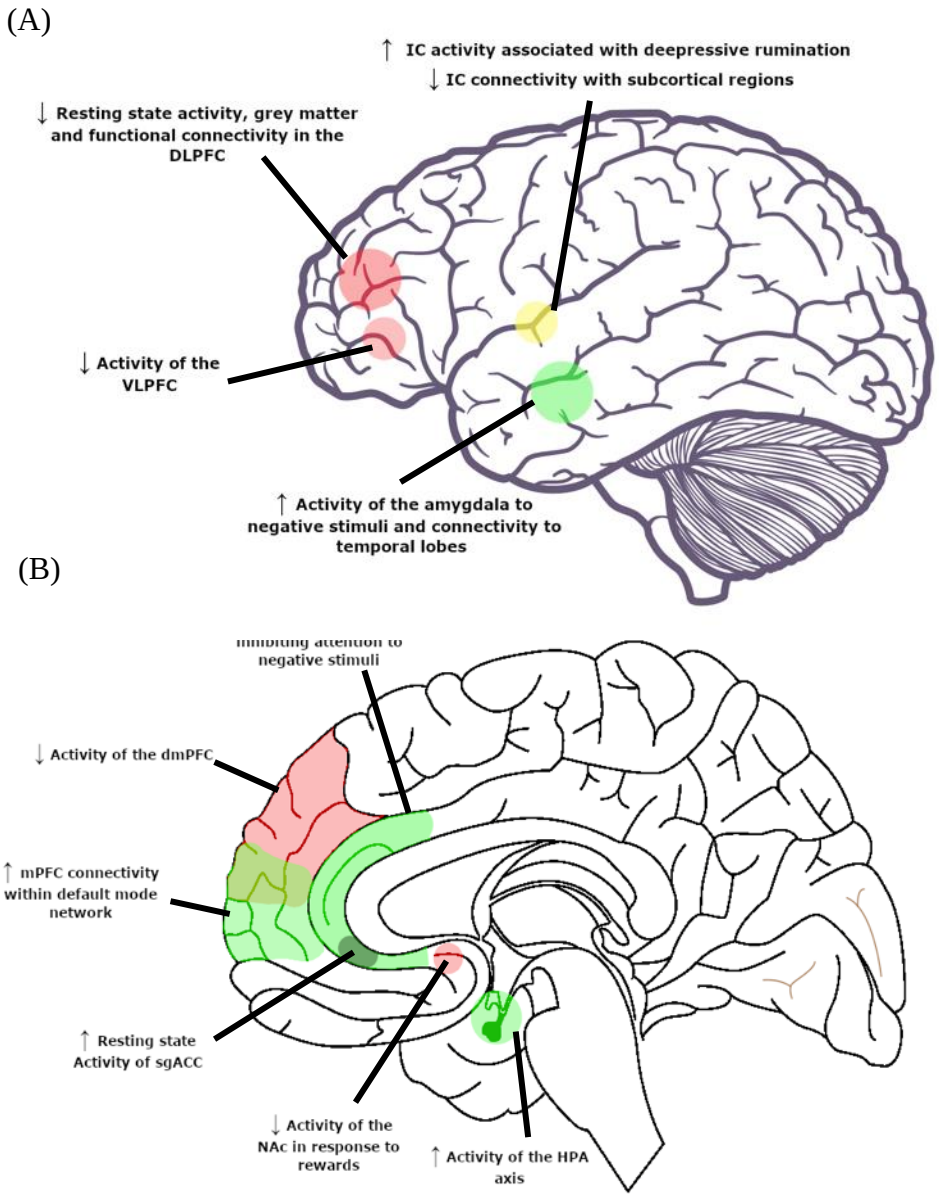

Figure 1. Brain Differences in Depression

Brain regions involved in emotion regulation affected individuals with MDD in (A) lateral view (adapted from doi.org/10.5281/zenodo.3925989) and in (B) medial view (adapted from 10.5281/zenodo.4312476). Green and red regions indicate overactivation and hypoactivity respectively, compared to healthy individuals. Adapted from "The neural systems of emotion regulation and abnormalities in major depressive disorder" by Park et al, 2019, Behavioural Brain Research. Brain outlines were downloaded from a free repository (www.scidraw.io.).

TMS to Treat MDD

Repetitive TMS (rTMS) is a non-invasive technique that has shown encouraging results in treating MDD. In TMS, a magnetic coil is placed on the dorsolateral prefrontal cortex (DLPFC) and magnetic pulses are delivered (see **Figure 2**). This generates long-term changes in the cerebral activity of systems involved under the area of stimulation (Magavi et al., 2017). Unlike ECT, rTMS does not cause significant side effects or cognitive sequela, or relevant adverse consequences such as tardive seizures, cognitive impairment, or confusion (Magavi et al., 2017). The most common method of stimulation is high frequency (HF) rTMS to the left DLPFC using a figure-of-eight coil. Generally, patients receive 1200-1500 10Hz pulses per session, grouped into 2-4 second train intervals ('on time') with 20-30 second intertrain intervals ('off time') (Lefaucheur et al., 2020; McClintock et al., 2018). The combination of shorter trains and relatively longer intertrain intervals is associated with increased safety. Sessions last for 30-40 minutes, and standard strategy comprises 10 to 30 treatment sessions over the course of 3 to 6 weeks (Lefaucheur et al., 2020; McClintock et al., 2018). High-frequency pulses are thought to excite neurons, which are hypoactive in the left DLPFC in patients with depression (Borrione et al., 2019; Pitsillou et al., 2020). About fifty experiments using rTMS to the left DLPFC in adults with treatment-resistant depression (TRD) have been performed since 1996, following very heterogeneous protocols (Lefaucheur et al., 2020). Two randomized well-controlled studies with sample sizes of 199 and 301 patients respectively (George et al., 2010; O'Reardon et al., 2007) showed that HF rTMS of the left DLPFC has antidepressant effect in patients with TRD. rTMS as a treatment for psychiatry disorders in adults has been approved by Health Canada and by the Food and Drug Administration (FDA) in 2002 and 2008 respectively (Leggett et al., 2014). Additionally, the CANMAT guidelines together with the Alberta Health Technology

Assessment consider high frequency (10 Hz) rTMS on the left DLPFC an effective treatment for adults with depression (Milev et al., 2016; Leggett et al., 2014). Other publications show valid justification for using low frequency (LF) stimulation of the right DLPFC, or bilateral stimulation (HF in the left DLPFC and LF in the right DLPFC). FDA has recently accepted deep rTMS utilizing a H1-coil to treat MDD, as it produces equivalent results to superficial rTMS (Lefaucheur et al., 2020).

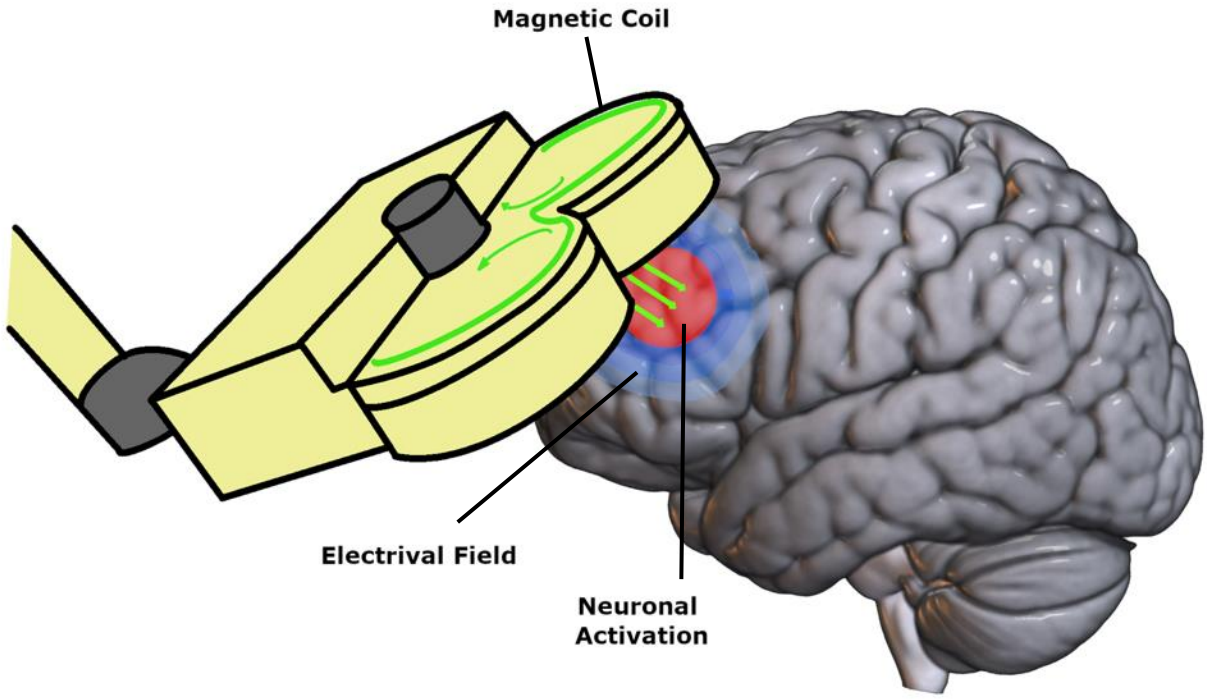

Figure 2. Schematic of The Application of TMS

Representation of the application of TMS on the left dorsolateral prefrontal cortex (DLPFC). A figure-of-eight coil is utilized to induce electric currents in the brain. Adapted from the press release from neuroCare Group (2017).

In the pediatric population, articles addressing the application of rTMS as a treatment for TRD are less abundant, and therefore the FDA has not yet approved the use of rTMS for adolescent depression. Nonetheless, there is evidence of beneficial effects of this technique in youth with several mood disorders, including MDD (McClintock et al., 2018). In fact, age is negatively correlated with clinical efficacy in adults with MDD, with rTMS being more effective the younger they are (Fregni et al., 2006). Similar to adults, TMS is a safe and tolerable procedure for children and youth, with headache being the most common side effect (experienced in 11% of cases) (Zewdie et al., 2020). The American Academy of Child and Adolescent Psychiatry (AACAP) suggests using rTMS treatment for 6-12 months in children and adolescents with depression, although significant variety is found in the literature (Narang et al., 2019). In the past decade, approximately ten studies have examined the effect of rTMS in adolescents with depression with promising results. MacMaster et al. (2019) conducted an experiment with 32 adolescents with moderate-to-severe TRD aged 13-21 in the Alberta Children's Hospital (ACH), which is the first pediatric TMS lab in Canada. This is the largest rTMS study in TRD pediatric population. After receiving rTMS for 15 consecutive weekdays, 56% of subjects presented a 50% or more decrease in the Hamilton Depression Rating Scale 17 items (Ham-D_{17}) score. The Ham-D_{17} is the main depression assessment scale in clinical settings and evaluates 17 different symptoms of depression in a structured interview format (Hamilton, 1960). The outcomes in MacMaster et al. (2019) support the use of rTMS in adolescent depression, but more studies are needed to optimize protocols and stimulation parameters for this specific age group.

Very recently, Dr. Croarkin and his lab published the largest study investigating the efficacy and safety of HF rTMS in adolescents (12-21 years old) with MDD (Croarkin et al., 2021). It was a double-blind randomized sham-controlled trial with 48 individuals receiving TMS by the 5

centimetres rule targeting approach and 55 participants assigned to sham. The results showed that although there was a significant decrease in the Ham-D 24 items score at the end, this change occurred in both the treatment and the sham group with no significant differences. This suggests that the antidepressant effect of TMS in the adolescent group could be due to placebo and has an important impact in this field of research. Future studies should work on reducing the placebo effects and re-examine the efficacy of TMS in adolescents with depression. In terms of safety outcomes, no tolerability issues emerged, and only relatively minor adverse effects appeared without compromising the safety of the patients.

Targeting Approaches for TMS

The left DLPFC, involved in higher-order cognitive processes and executive functions, is a relatively large structure with a volume of approximately 9 cm^3 (Sanches et al., 2009). It has a surface area of about a playing card with differing projections based on where you are in the DLPFC. Many targeting approaches to determine the rTMS stimulation site in the DLPFC in MDD have been used including the 5 centimetres rule, electroencephalogram (EEG) landmarks (F3 and F5), Broadmann Areas 9 and 46 (BA9 and BA46), their junction point, and the middorsolateral prefrontal cortex (see the location of these sites in **Figure 3**). The conventional "5-centimetre rule" (5 cm rule) identifies the hand motor hotspot, usually defined at the first dorsal interosseous (FDI) muscle of the contralateral hand (i.e. right FDI for left primary motor cortex or LM1 and left FDI for right primary motor cortex or RM1), and then the stimulation target site is determined to be 5 cm anterior to this hotspot (see **Figure 4**). However, this method has been shown to be inaccurate as the left DLPFC appears to be more anterior in most

individuals at about 7 cm from the hotspot. In fact, Herbsman et al. (2009) showed that the more anterior and lateral the coil was placed using the conventional 5 cm rule, the better the outcome was in adults with depression. Another method for positioning the coil is based on the F3 standardized electroencephalogram (EEG) landmark using the International 10-20 System for placement of electrodes. The F3 EEG approach is more precise than the 5 cm rule because it accounts for cranial size and shape. Similarly, Rusjan et al. (2010) used the F5 EEG landmark. Other targeting approaches involve coordinates centered on Broadmann areas (BA) 9, 46, and the junction between these two using neuronavigation (3D brain rendition from template or individual MRI data). A target-comparison study showed that stimulation at the junction between BA9 and BA46 had an increased antidepressant effect compared to the standard 5 cm rule procedure. These results suggest that the location of the rTMS stimulation site is very relevant when it comes to treatment efficacy, and that more anatomically accurate approaches seem to lead to an increased rTMS response. However, rationale regarding why some sites might produce more favorable outcomes is lacking (Lefaucheur et al., 2020; Pitsillou et al., 2020).

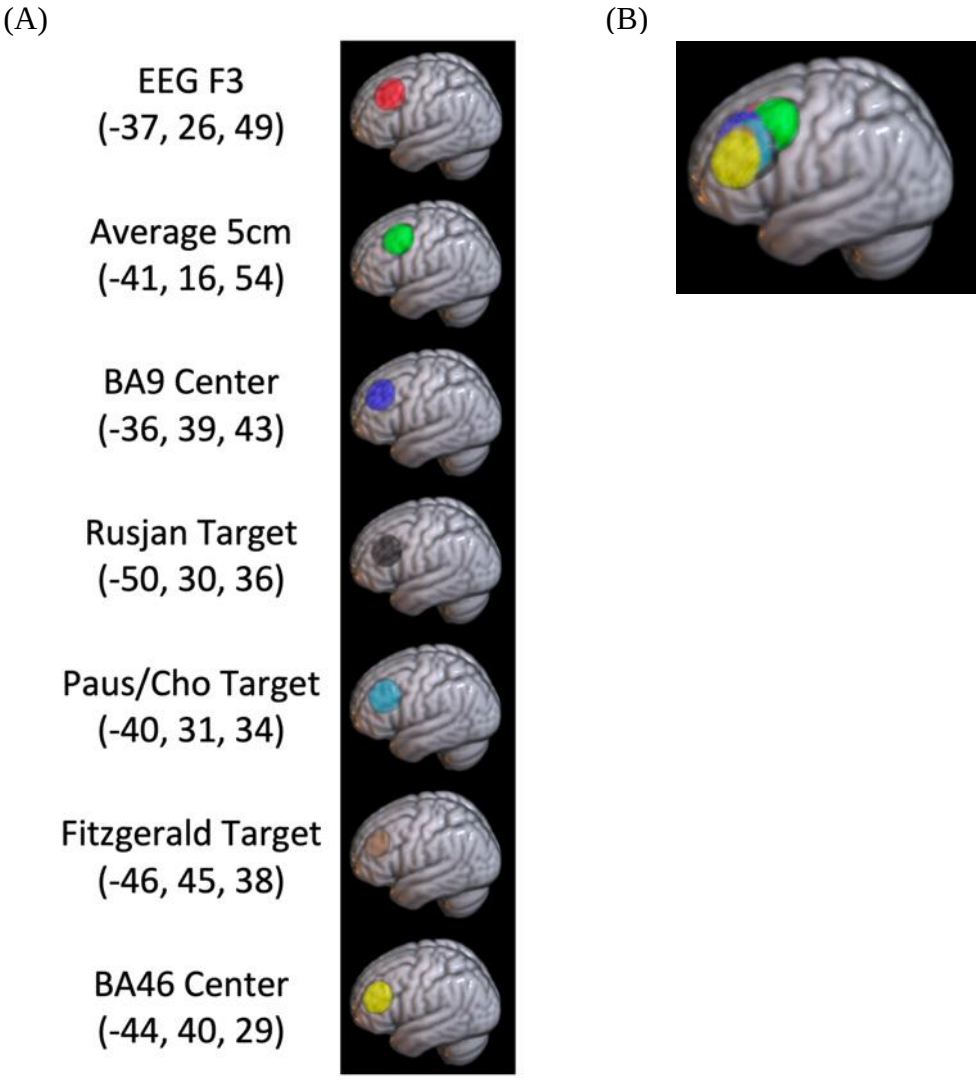

Figure 3. Targeting Approaches

Representation of the 25mm spheres used as regions of interest (ROIs) for each of the seven targeting approaches' sites in the DLPFC, (A) individually and (B) together. They are centered on the MNI coordinates provided in Fox et al. (2012) paper. MRIcroGL software was used to display the ROIs.

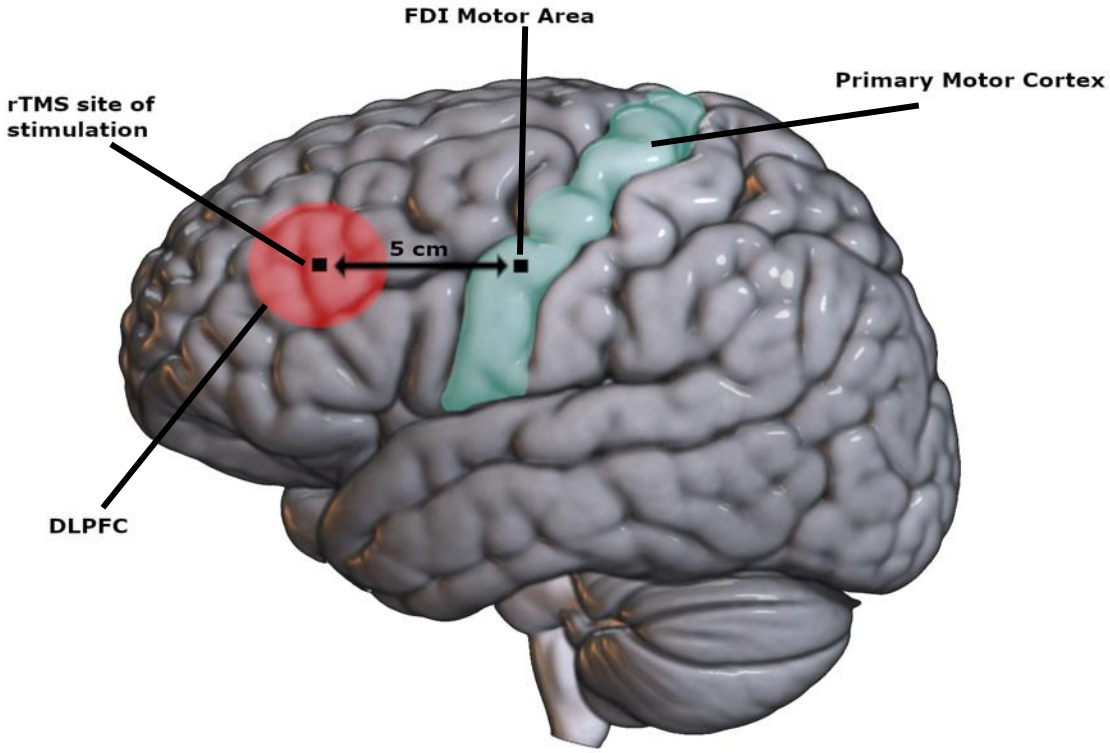

Figure 4. Schematic of the 5cm rule

Illustration of the TMS coil location using the 5 centimetre-rule targeting approach. First, the coil is applied to the first dorsal interosseous muscle (FDI) in search of the FDI motor hotspot, which determines resting motor threshold (RMT). Then, the coilThe coil is then moved 5 cm anteriorly to target the DLPFC. Adapted from Sokhadze et al. (2018).

Fox et al. (2012) and Functional Connectivity

In 2012, Fox et al. proposed a novel targeting technique to treat adults with treatment-resistant depression. They hypothesized that the differences in treatment efficacy could be related to the changes in functional connectivity between the rTMS stimulation site and an area heavily affected in depression: the subgenual anterior cingulate cortex (sgACC) or subgenual cingulate.

For a clear understanding, background regarding functional connectivity in resting-state imaging is given in the next paragraph.

The brain is divided into different functional networks that encompass regions that cooperate together to perform a given task (Liston et al., 2014). Even though these networks were originally identified by observing changes in brain activity during task performance, similar relationships are consistent at rest and thus, are represented intrinsically in the brain (Fox and Raichle, 2007). In resting-state circumstances, the correlation between spontaneous fluctuations in the blood oxygen level-dependent (BOLD) signal is examined to determine the intrinsic functional connectivity between two given regions (Fox et al., 2005). With this being said, two areas expressing high positive correlation during resting-state imaging, have similar and simultaneous fluctuations of activity during a significant part of the scan time. Therefore, it can be said that they have a high functional connectivity and they are part of the same intrinsic network (Chen et al., 2011). On the other side, large negative correlations (or anticorrelations) denote opposite activation patterns throughout the resting-state scan. The actual meaning of these negative correlations between brain regions and their functional relationship is still unclear (Parente and Colosimo, 2018).

Two important intrinsic networks in the brain that show consistent abnormalities in depression are the default-mode network (DMN) and central-executive network (CEN), which includes the DLPFC (Liston et al., 2014). As we have already mentioned, the DLPFC appears to be consistently hypoactive in patients with MDD, making DLPFC the focus of TMS targeting for depression. Another recurrent finding in MDD is the increased correlation or abnormal connectivity patterns between several areas of the DMN and the subgenual cingulate (Greicius

et al., 2007). The sgACC is a key brain region in the affect (or emotion) regulation system as it has connections to both the limbic system and the cognitive control network (Scharnowski et al., 2020). In patients suffering from depression, sgACC is decreased in grey matter volume due to glial cells loss and is distinctively hyperactive (Drevets et al., 2008; Lichenstein et al., 2016). Additionally, individuals diagnosed with depression express a decreased functional connectivity between the sgACC and the DLPFC with respect to healthy controls (Chai et al., 2016). Although, this evidence mostly comes from data in adults, there a few studies showing similar results in relatively small samples of adolescents with MDD (Cullen et al., 2009, Gaffrey et al., 2010). Since several studies demonstrate that the activation level of sgACC is reduced after rTMS treatment, this technique could be evoking the antidepressant effects through the DLPFC-sgACC connections (Jing et al., 2020).

In Fox et al. (2012), they utilize this distinctive DLPFC-Subgenual functional relationship to optimize the rTMS targeting in adults with depression. In their study, they obtained the coordinates of rTMS stimulation sites from studies that had utilized seven different targeting approaches to find the DLPFC stimulation site: the standard 5 cm rule (average of Herwig et al., 2001 and Herbsman et al., 2009 coordinates), F3 EEG (Herwing et al., 2003), BA 9 (Rajkowska G et al., 1995), BA 46 (Rajkowska G et al., 1995), the junction between BA 9 and BA 46 (Fitzgerald et al., 2009), F5 EEG (Rusjan et al., 2009), and mid-dorsolateral prefrontal cortex (Paus et al., 2001 and Cho et al., 2009). Functional connectivity from these coordinates to the subgenual cingulate was determined in 98 control subjects. The FMRIB Software Library (FSL) was used to analyse resting-state functional connectivity MRI (fcMRI). The 5 cm and F3 EEG approach showed the weakest anticorrelation, whereas the Fitzgerald junction between BA9 and

BA 46 showed the strongest negative correlation. Data was extracted from Herbsman et al. (2009) and Fitzgerald et al. (2009) specifically and the results showed that the more anticorrelated a TMS target site was with the subgenual cingulate, the more efficient the rTMS therapy appeared to be in reducing depressive symptoms. Utilizing this information, Fox et al. (2012) generated an optimized left DLPFC target site for TMS by finding the location most anticorrelated with the subgenual cingulate. The authors applied this connectivity analysis to 13 individuals (aged 18-65 years) with MDD, including the optimized site coordinates, and showed that better clinical efficacy was related to a higher anticorrelation between the stimulation site and the subgenual cingulate. As a consequence, they support the use of a connectivity-based targeting approach to determine the rTMS stimulation site in adults with MDD.

Gaps in Literature and Rationale

According to the literature, the location of the site of rTMS stimulation to treat depression significantly affects the treatment response. However, among the many targeting approaches that have emerged in the last two decades, there is no evidence that justifies the use of one target site above the others. There is need for further optimization of TMS targeting strategy, especially in adolescents. Fox et al. (2012) suggested that individual connectivity patterns between the cortex and deeper subcortical structures could be used to identify a DLPFC optimized stimulation site. They called this method the "connectivity-based approach" and observed that the correlation in activity between the DLPFC and the subgenual cingulate was an efficient predictor of clinical efficacy in adults. However, there are no studies investigating this approach in the pediatric population. The purpose of this study is to (1) replicate Fox et al.

(2012) and determine the connectivity pattern using various targeting approaches in adolescents and (2) to determine if connectivity-based targeting method is associated with rTMS treatment in TRD youth. These aims will be achieved by analysing data that had been previously collected by the MacMaster research lab in adolescents with TRD. Results from this study will provide evidence for precise rTMS treatment targeting in children and youth suffering from depression.

Specific Aims and Hypothesis

Experiment 1: Target approach analysis

Aim 1. To replicate connectivity patterns based on targeting approaches described in Fox et al. (2012) in adolescents with depression. We will be using brain coordinates previously defined by Fox et al. (2012) for each target and the fMRI scans from both typically developing controls (TDC) and treatment resistant depression (TRD) adolescent populations (n=18 and n=37 respectively, ages 12-22).

Hypothesis 1. Akin to Fox et al. (2012), we hypothesize that all seven left DLPFC sites will express a negative correlation (anticorrelation) with the subgenual cingulate at rest. Among them, I expect BA46 and the Fitzgerald approach (junction between BA9 and BA46) to express the highest anticorrelation, and the F3 EEG and 5 cm rule to show the lowest anticorrelation.

Experiment 2: Functional connectivity and clinical efficacy

Aim 2. (2A) To determine if the strength of the connectivity between the individual rTMS coordinates at baseline and the subgenual cingulate is different in treatment responders (≥50%

decrease in Ham-D) versus non-responders; (2B) to determine if the strength of the connectivity between the individual rTMS coordinates and subgenual cingulate is associated with treatment response. We will use the fMRI data from a population of youth with TRD who completed 3-weeks (15 sessions) of rTMS treatment (ethics ID 24656; REB15-0970_REN3) and the clinical outcome from the 17-item Hamilton Depression Rating Scale (Ham-D).

Hypothesis 2. We hypothesize that responders will show a higher anticorrelation with the subgenual cingulate than non-responders at baseline. Overall, we expect that the larger the anticorrelation between rTMS stimulation site and the subgenual cingulate the greater the reduction in Ham-D score, suggesting a more efficient treatment protocol. In other words, the decrease in Ham-D score will be higher when the anticorrelation is larger.

CHAPTER 2: METHODOLOGY

Participants

This study used the data collected in our lab and published recently (MacMaster et al. 2019). A total of 39 adolescents diagnosed with treatment-resistant depression (TRD) in the Alberta Children's Hospital were originally recruited. The inclusion criteria included being 12-22 years old, having an MDD diagnosis based on the Kiddie Schedule for Affective Disorders and Schizophrenia Present and Lifetime version (K-SADS-PL), having failed to respond to at least one SSRI trial and have the ability to give verbal consent. Out of the 39 participants with TRD, 37 (15 F, 22 M, mean age 17.4 ± 2.1) underwent baseline brain imaging acquisition, and 32 (15 F, 17 M, mean age 17.9 ± 2.0) completed rTMS treatment. The Hamilton Depression Rating Scale 17 items (Ham-D_{17}) (Hamilton, 1960) was used for depression assessment before and after treatment as described in detail in MacMaster et al. (2019). Eighteen adolescents (13 F, 5 M, mean age 17.7 ± 2.6) without MDD were recruited as typically developing controls (TDC) after the K-SADS-PL interview.

According to the Ham-D scores pre-treatment (baseline) 5 of 32 individuals with TRD were rated as having mild depression, 9 as moderate, 4 as severe, and 14 as very severe. Psychotropic pharmacology was allowed if medication type and dosage was constant for at least 6 weeks before study participation, with the intention to stay constant throughout the trial. Ten (31.25%) participants were not taking any medication, 14 were having SSRIs, 7 norepinephrine and dopamine reuptake inhibitors (NDRIs), 4 serotonin and norepinephrine reuptake inhibitors (SNRIs), 3 atypical antipsychotics, 1 benzodiazepines, 1 guanfacine, 1 lithium, 1 opioid analgesics, 1 antibiotic, 1 tetracyclic antidepressant, and 1 serotonin antagonist and reuptake

inhibitors (SARIs). No participants modified their medication or dosage during the three weeks of rTMS intervention. Eighty-eight percent of participants reported comorbidities: 24 showed generalized anxiety disorder (GAD), 10 social phobia, 8 panic disorder, 4 attention deficit hyperactivity disorder (ADHD), 3 social anxiety disorder, 2 post-traumatic stress disorder (PTSD), 2 specific phobias, 1 separation anxiety disorder, 1 conduct disorder, 1 bulimia, and 1 Ehler-Danlos syndrome. Some individuals reported more than one comorbidity.

MRI Acquisition

Baseline anatomical T1-weighted and resting-state functional magnetic resonance imaging (rsfMRI) scans were acquired for 18 TDCs and 37 patients with TRD. Scans were collected at the Alberta Children's Hospital with a General Electric (GE) Healthcare Discovery MR750w 3.0T Magnetic Resonance scanner using a 24-channel head coil. During the resting-state fMRI, subjects were asked to "be still, look at the cross and think of nothing in particular" (dark cross on grey screen). Resting-state whole-brain fMRI scans were collected for 5 minutes using an echo-planar imaging (EPI) mode under these parameters: TR = 2,000 ms, TE = 30 ms, flip angle = 90º, number of slices = 36, total volumes = 150, voxel size = 3.6 x 3.6 x 3.6 mm^3, interleaved bottom-up acquisition, field of view = 230 mm 64 x 64 matrix.

Axial T1-weighted fast spoiled gradient echo (FSPGR) brain volume (BRAVO) was acquired with the following parameters: TR = 8.27 ms, TE = 3.15 ms, TI = 600 ms, flip angle = 10º, number of slices = 226, voxel size = 0.46 x 0.46 x 0.80 mm^3, 300 x 300 matrix.

RTMS Intervention

The TRD group received 15-sessions of rTMS to a left DLPFC target determined through the 5-cm rule. A Magstim SuperRapid^2, air cooled 90mm figure-of-8-coil connected to a Magstim 200 stimulator (Magstim, Dyfed, UK) was used for rTMS treatment delivery. Resting motor threshold (RMT) of the left motor cortex (LM1) was determined by the right FDI muscle. RMT was defined as the minimum intensity of stimulator output required to cause motor-evoked potentials (MEP) of ≥50 μV in at least 5 of 10 trials (Kirton et al., 2010). The DLPFC target was located by the 5 cm rule approach, in which the coil was moved 5 cm anterior along the scalp following the line between the nasion (most anterior point of the frontonasal suture) and the hotspot, and the target was anatomically confirmed and adjusted using neuronavigation of each participant's 3D MRI (Brainsight2, Rogue Research, Montreal). The TMS coil was placed laterally at 45 degrees to the midsagittal line for both RMT determination (at the LM1) and treatment target site (left DLPFC).

Participants received high frequency (10Hz) rTMS for 15 consecutive weekdays for 37.5 minutes each day (120% RMT, 75 trains of 4 seconds, intertrain interval 26 seconds, 3,000 pulses). Passive activities during rTMS sessions were performed, including watching movies or listening to music.

MRI Processing and Analysis

The present study utilized the FMRIB Software Library (FSL) version 6.0.3 for fMRI preprocessing and first-level analysis. Preprocessing steps were based on methods described in

previous studies (Fox et al. 2012, Fox et al. 2005 and Van Dijk et al. 2010) and are described below.

Experiment 1: Target approach analysis

The anatomical and functional MRI scans acquired at baseline (pre-treatment, 18 TDCs and 37 individuals with TRD) were used to determine the connectivity between the various target site options (as presented in Fox et al., 2012) and the subgenual cingulate. A total of eight regions of interest (ROIs) were defined a priori for this analysis, the subgenual cingulate ROI and the DLPFC ROIs for the seven targeting approaches: (1) F3 EEG, (2) 5 cm rule (average), (3) BA9 Center, (4) Rusjan Target, (5) Paus/Cho Target, (6) Fitzgerald Target, and (7) BA46 Center. Coordinates were converted from MNI space to voxel location using FSLeyes. Then, 10 mm and 25mm spheres were created centered on the subgenual cingulate and on the DLPFC coordinates, respectively. The subgenual cingulate ROI is located in the right hemisphere and the DLPFC ROIs in the left. Spheres were masked to exclude voxels outside grey matter using the Harvard/Oxford atlas available in FSL, thresholded at an intensity of 70. Additionally, we used the Harvard/Oxford atlas to generate masks for deep white matter and lateral ventricles, which were later removed as sources of noise in first-level analysis.

Preprocessing: First, for each participant's scan, non-brain tissue was eliminated by robust brain centre estimation using the Brain Extraction FSL Tool (BET). Second, through the FEAT function the following preprocessing steps were performed to reduce artifacts: the first 4 volumes of the functional scan were deleted, high pass filter cut-off of 100 seconds and spatial smoothing at 6 mm full-width at half-maximum were applied, and interleaved slice timing

correction was selected. The intra-modal motion correction tool MCFLIRT was selected. As a consequence, six motion parameters computed by rigid body and rotation during preprocessing were created. They were later used in First-Level Analysis to account for motion. Last, the intensity values of the preprocessed image were scaled to 1000 as described in Fox et al. (2005).

Registration and Noise Time Series Extraction: Linear and non-linear transformations were applied to the scaled filtered functional images generated after preprocessing using the FLIRT and FNIRT toolboxes respectively. Next, the registered functional images were used to extract time series for the sources of noise, i.e., mean whole-brain signal or global signal (using a binarized MNI standard image as mask), lateral ventricles, and deep white matter.

Motion Detection: Using the *fsl_motion_outliers* tool, the framewise displacement (FD) of the preprocessed fMRI volumes (n=146 volumes) for each subject was calculated. FD is measure of volume-to-volume changes in head position. We set a threshold at a FD of 0.5 mm and obtained one confound matrix per participant containing the volumes with a FD above the threshold (outliers). This matrix was later used for patient exclusion and volume censoring in the next step.

Noise Removal and ROIs Time Series: The sources of variance (the six motion parameters, global signal, lateral ventricles signal and deep white matter signal) were removed by linear regression utilizing the FEAT tool in FSL. Each source was included as a different explanatory variable (EV). Moreover, the motion confound matrix was inserted as additional EV in the model to censor those volumes with excessive head position change (outliers). To the residual image generated after this step, we added the mean signal. The outcome was used to extract the time series of the Subgenual ROI and the seven DLPFC ROIs.

Quality check: The raw functional and anatomical images, the outcome of the brain extraction and reorientation steps and the registered image were individually reviewed for quality. Those individuals with a lack of fMRI scan, signal drop or extreme signal homogeneity were excluded from functional connectivity mapping and data analysis. Additionally, participants with more than 30 outliers (one minute of data) in the confound matrix for head motion were also excluded from the analysis. A total of eight participants (6 patients and 2 controls) were excluded.

Functional Connectivity Coefficients: R programming language was used to calculate the strength of functional connectivity (and its significance) between each of the DLPFC ROIs and the Subgenual Cingulate ROI by using Pearson correlations. Once this was calculated for each participant and targeting approach, the average, standard deviation and standard error was calculated for TRD and TDC groups independently. A one-sample t-test was used to determine whether the mean correlations were showing a significant connectivity between a specific targeting region in the DLPFC and the subgenual cingulate (i.e., significantly different from 0). Afterwards, we measured if there were any significant correlations between DLPFC-Subgenual connectivity and age, and between DLPFC-Subgenual connectivity and biological sex (after testing for homogeneity of sex distribution with a chi-squared test). One-way repeated measures ANOVA was used to observe if the average correlation values for each targeting approach were significantly different. Last, two-sample t-tests were used to identify significant differences between the average correlations in the TRD versus the TDC groups.

Functional Connectivity Maps: This last step is aimed to create seed-based correlation maps to show the correlations visually. To do them, the FEAT tool in FSL was again utilized at the individual level. Statistical correlation analysis was performed between the targeting

approaches' sites and the rest of the brain by inserting the time series of the DLPFC ROIs as the only EV in the model. Two contrasts were applied to obtain both positive and negative correlation images. The MNI standard was used as a pre-threshold masking to eliminate correlation values from outside the brain. Images were thresholded at $p<0.001$ uncorrected as used in (Fox et al, 2012). Later, the thresholded images (or maps) of positive correlation for each ROI were merged to create a 4D image including the participants of a specific group (TRD or TDC). For instance, EEGF3 positive correlation images were merged for participants with TRD and controls, respectively. Similarly, merged images for EEGF3 negative correlation maps and repeated for the other 6 ROIs. Last, one-sample t-test was performed to create the final connectivity maps for each targeting approach. These maps were thresholded at $t = 1.7$ ($p<0.05$) for visualization.

More methodological details can be found in the

Chapter 5: section. This includes **Table 4**, which shows the specific input and output files for the subject-level analysis.

Experiment 2: Functional Connectivity and Clinical Efficacy

For experiment 2, the structural and functional scans at baseline from the 32 participants with MDD who underwent TMS were used (5 participants withdrew or were excluded before TMS intervention finished). Participants excluded in experiment 1 due to poor image quality or excessive motion were also excluded for experiment 2. We also utilized the percentage change in Ham-D of these individuals from baseline (pre-treatment) to post-treatment. The individual

coordinates of the rTMS stimulation site in the DLPFC were first converted from world coordinates to voxel coordinates using RStudio (*Rnifit*, *fslr* and *oro.nifti* packages). An individualized 10 mm sphere ROI centered on the individual stimulation site was created. Following the same steps as experiment 1, the functional connectivity strength from the individual DLPFC stimulation sites to the subgenual cingulate were calculated. Then, to address aim 2A, a two-sample t-test was used to calculate significant differences between DLPFC-Subgenual correlation in responders (≥ 50% decrease in Ham-D scores) versus non-responders. For aim 2B, the correlation coefficient between the DLPFC-Subgenual connectivity and the Ham-D % change for each patient was calculated. Our significance threshold was at $p<0.025$ (one-tailed). We also identified possible outliers and extreme points in the dataset.

CHAPTER 3: RESULTS

Experiment 1: Target Approach Analysis

Final Sample: Out of the 37 participants in the treatment group, we excluded 2 due to poor quality of the functional scan and 4 due to excessive movement in head position (more than 30 volumes were outliers). Among the 18 participants in the control group, 2 participants were excluded due to a lack of an fMRI scan and an excess of head movement respectively. The final sample for experiment 1 included 31 patients with TRDs (13 F, 18 M, mean age 17.7 ± 2.1) and 16 TDCs (11 F, 5 M, mean age 18.0 ± 2.4). The groups did not differ in age (t = -0.40, df = 26.84, p = 0.69) or sex distribution (χ^2 = 2.06, p = 0.15).

Functional connectivity: The Pearson Correlation between the seven targeting approaches' regions and the subgenual were calculated successfully for the 31 participants with TRD and 16 controls, generating a total of 217 and 112 correlation values respectively. Among them, 33% (TRD group) and 21% (TDC group) of the correlations indicated that there was significant linear relationship between the activity patterns of the targeting approach and subgenual ROIs at an alpha value of 0.05. Later, these values were grouped by targeting approach. The values of the mean correlations, standard deviations and standard errors of the mean for each targeting approach are displayed in

. For the TRD group, Rusjan, BA46 and Paus ROIs show an overall anticorrelation with the subgenual cingulate, whereas Fitzgerald, 5 cm rule, EEGF3 and BA9 techniques showed a positive correlation on average (see **Figure 5A**). For the TDC group, the mean r values are more negative than in the individuals with treatment-resistant depression. BA46, Rusjan, Paus and Fitzgerald are anticorrelated, and 5 cm rule, BA9 and EEGF3 are positively correlated with the subgenual (see **Figure 5B**). Three targeting approaches in the TRD group (EEGF3, Avg5 and BA9) showed a mean positive functional connectivity to the subgenual that is significant at a confidence level of 95%. Similarly, three in the TDC group (Rusjan, Paus and BA46) have a significant mean negative functional connectivity (see the asterisks in **Figure 5**). The functional

connectivity maps between the subgenual cingulate and the DLPFC ROIs are also included in **Figure 5**. The one-way repeated measures ANOVA showed that the majority of the differences between two DLPFC-Subgenual mean correlations from two given targeting approaches were significant in the TRD group. Contrarily, in the TDCs, most of the mean correlations from distinct targeting approaches were not significantly different (see

Table 3). The two-sample tests showed that given a specific targeting approach, the mean correlation was not significantly different between patients and controls (p>0.01).

Table 2. Mean Correlation, Standard Deviation and Standard Error.

For each of the seven targeting approach, the mean Pearson Correlation (r) between the targeting approach and subgenual ROIs are displayed, together with the standard deviation and the standard error of the mean.

	TRD Group			TDC Group		
	Mean Correlation	**Standard Deviation**	**Standard Error**	**Mean Correlation**	**Standard Deviation**	**Standard Error**
EEGF3	0.102	0.126	0.023	0.043	0.102	0.025
Avg 5	0.064	0.149	0.027	0.010	0.147	0.037
BA9	0.114	0.138	0.025	0.039	0.099	0.025
Rusjan	-0.058	0.168	0.030	-0.110	0.115	0.029
Paus	0.000	0.167	0.030	-0.063	0.108	0.027
Fitzgerald	0.031	0.156	0.028	-0.031	0.114	0.029
BA46	-0.052	0.166	0.030	-0.114	0.117	0.029

(A)

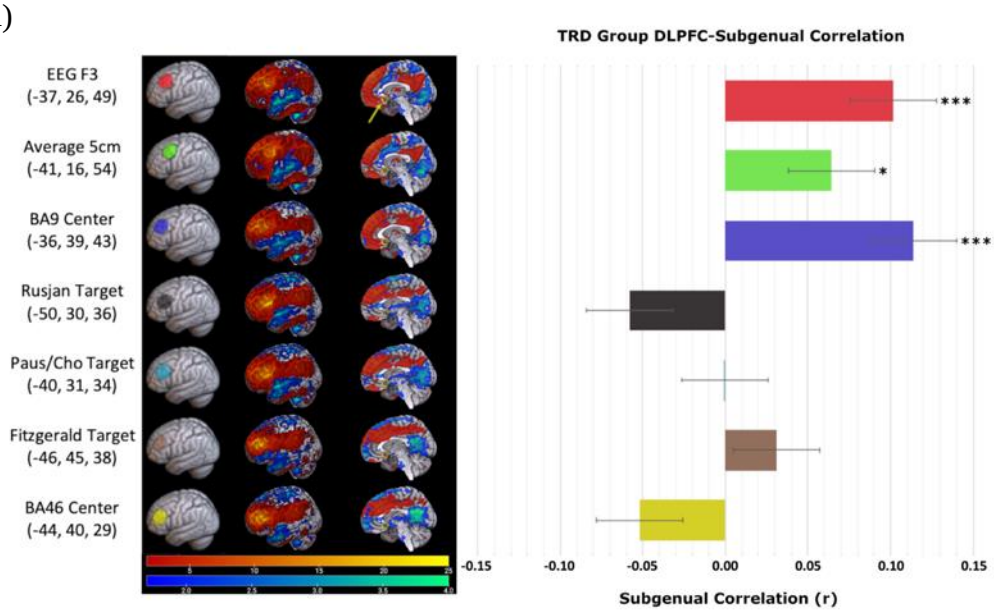

(B)

Table 3. One-way Repeated Measures ANOVA Results.

Significance of the difference between the mean DLPFC-Subgenual correlation of two given targeting approaches (named target 1 and 2 in the table) after the one-way repeated ANOVA statistical test.

Target 1	**Target 2**	**TRD Group Significnace**	**TDC Group Significance**
Avg5	BA46	*	ns
Avg5	BA9	ns	ns
Avg5	EEGF3	ns	ns
Avg5	Fitgerald	ns	ns
Avg5	Paus	ns	ns
Avg5	Rusjan	**	ns
BA46	BA9	****	***
BA46	EEGF3	****	**
BA46	Fitzgerald	****	****
BA46	Paus	*	ns
BA46	Rusjan	ns	ns
BA9	EEGF3	ns	ns
BA9	Fitzgerald	***	ns
BA9	Paus	****	***
BA9	Rusjan	****	***
EEGF3	PFitzgerald	ns	ns
EEGF3	Paus	***	**
EEGF3	Rusjan	****	***
Fitzgerald	Paus	ns	ns
Fitzgerald	Rusjan	***	*
Paus	Rusjan	****	***

Note. * indicates $p<0.05$, **indicates $p<0.01$, *** indicates $p<0.001$, **** indicates $p<0.0001$, *ns* indicates “not a significant difference”.

Experiment 2: Functional Connectivity and Clinical Efficacy

Final Sample: 5 patients with MDD did not undergo rTMS due to withdrawal or exclusion (MacMaster et al., 2019). Therefore, 32 participants completed all the rTMS sessions. These patients were assessed by Ham-D before and after treatment. The 6 MDD patients excluded in experiment due to poor quality and excessive head motion, were also not included in the analysis for experiment 2. Thus, the final sample for experiment 2 consisted of 26 patients with treatment-resistant depression (13 F, 13 M, mean age 17.9 ± 1.8).

Results: Out of the 26 individuals, 15 had a 50% or higher reduction in Ham-D scores and thus were categorized as responders. The other 11 patients were non-responders. There was no significant difference in age ($t = 0.28$, $df = 21.29$, $p = 0.78$) or sex-distribution ($\chi^2 = 2.52$, $p = 0.11$) between responders and non-responders. Two-sample t-test showed that there was no significant difference in DLPFC-Subgenual connectivity in responders compared to the non-responders ($t = -1.53$, $p = 0.15$). Correlation between clinical efficacy (Ham-D % change) and DLPFC-subgenual connectivity indicated a positive association ($r = 0.39$, $p = 0.051$) (see **Figure 6**). This correlation is significant at an alpha value of 0.025 (one-tailed). Additionally, we can say that 15% of the variability in Ham-D % change can be explained by the subgenual correlation. By observing the data distribution, one data point was identified as an outlier although there were no extreme points. Even though the outlier did not change the direction of the correlation, the strength of the correlation was reduced (see **Figure 8**).

(A)

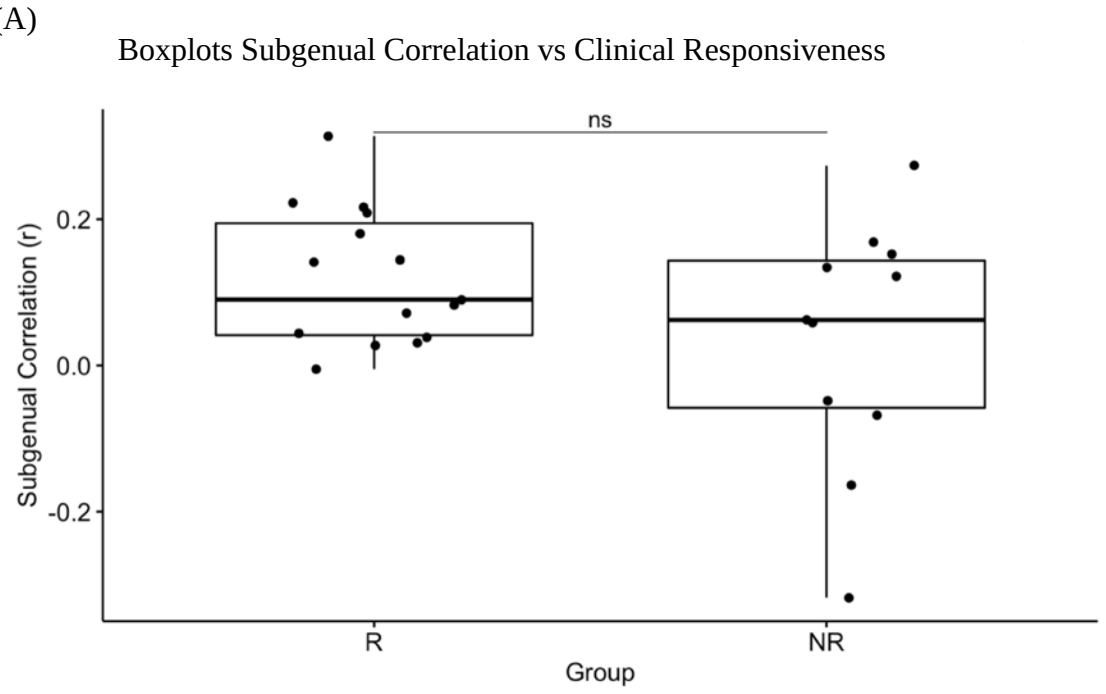

(B)

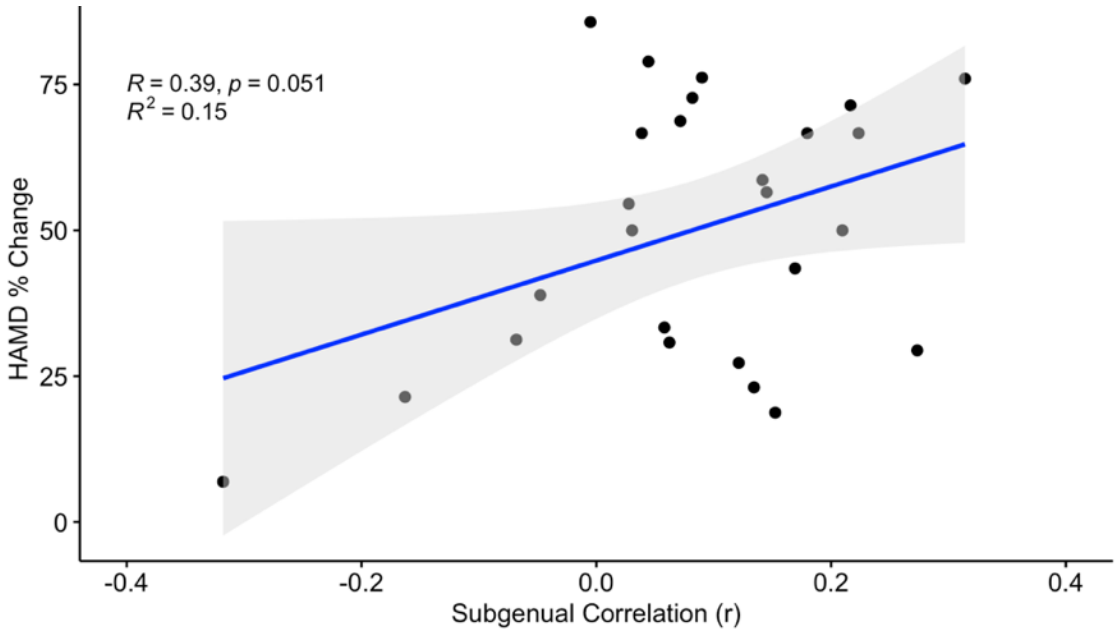

Figure 6. Functional Connectivity and Clinical Efficacy

(6A) Box plots depicting subgenual-DLPFC connectivity for rTMS treatment responders (R) and non-responders (R). There were no significant differences between the groups (ns, $p > 0.05$). (6B) Correlation between the % decrease in Ham-D scores (clinical efficacy) and the subgenual connectivity. The coefficient of correlation (R) with its p-value and the coefficient of determination (R^2) are displayed in the graph. Grey area: 95% confidence interval for the linear fit.

CHAPTER 4: DISCUSSION

Overview and Comparison to Fox et al. (2012)

In this study, we examined the novel connectivity-based targeting approach in children and adolescents. We did so by replicating and extending some of the experiments performed by Fox et al. (2012) in a pediatric group. An important asset of our work is that our sample includes both typically developing controls and youth with TRD that underwent rTMS treatment. The outcomes show some contradictions if they are compared to the adult sample of Fox et al. (2012). Unlike their work, where all seven DLPFC ROIs were negatively correlated, our TRD group had three DLPFC ROIs positive correlated to the subgenual cingulate. Similarly, in our control group, DLPFC-Subgenual positive correlations were noted in 4 out of the 7 targeting approaches. Secondly, as opposed to the results in Fox et al., higher positive correlation (and not negative) between DLPFC and subgenual was significantly associated with greater clinical efficacy (% decrease in Ham-D scores).

In the sections below, we will be discussing the meaning of these results by comparing our outcomes to those found in literature and referring to the neurobiology of depression. We will also mention the limitations that we have encountered, as well as the future work that could positively complement this research project. Finally, we will sum up the main points in the

Conclusion section.

DLPFC-Subgenual Connectivity in Adolescents

A Precise Targeting Method

Since the first use of TMS to treat depression at the end of the 20th century, many targeting protocols have been proposed (Lefaucheur et al., 2020). The 5 centimetres rule approach is the most common one and although it is very practical, it does not account for individual differences in brain size, morphology and functional connections (Jing et al., 2020). Apart from the 5 centimetres rule, other techniques have arisen, including the F3 and F5 EEG landmarks, and those based on the Broadmann Areas, among others (Herbsman et al., 2009; Rusjan et al.,2010). The literature shows a great variability in the efficacy of rTMS with changes in the location of the stimulation site (Lefaucheur et al., 2020; Pitsillou et al., 2020). The large variability among the sites of stimulation in the DLPFC is what motivated Dr. Fox and his lab to examine the DLPFC-Subgenual connectivity of seven different targeting regions and eventually correlate it to the clinical efficacy. We followed the methods described in Fox et al. (2012) to study this approach in a pediatric population. Our first experiment shows that most of the DLPFC-subgenual correlations happened to be different from one another in the TRD group. This supports the fact that the brain activity in the DLPFC can significantly differ even in very proximal sites, and thus, every point is distinctly connected to other regions of the cortex and deep limbic structures such as the subgenual cingulate. These differences reinforce the importance of precisely defining the stimulation target (Jing et al., 2020). Nevertheless, we did not find many differences in the DLPFC-Subgenual connectivity in the seven targeting approaches in the healthy group. This could be due to the reduced size of the TDC sample. Future studies should investigate how DLPFC-Subgenual correlation changes as we move the site of stimulation in a larger group of healthy adolescents.

Direction and Magnitude of DLPFC-Subgenual Connectivity

The direction of DLPFC-Subgenual correlations reported in experiment 1 were in disagreement with the initial hypothesis. Not all seven targeting approaches appeared to have a negative correlation with the subgenual. In fact, only Rusjan BA46 and Paus in the TRD group showed an anticorrelation. The functional relationship between DLPFC and the sgACC in the general population is not very clear in the literature. Whereas most of the articles state that these two regions maintain an anticorrelation in adults (Fox et al., 2012; Margulies et al., 2007), other studies show that, within the extension of the DLPFC, there are both positively and negatively correlated parts to the sgACC (Cole et al., 2020). Thus, since the coordinates we used in experiment 1 to define our DLPFC ROIs in our pediatric population were extracted from studies in adults, it could be possible that we ended up encompassing an area of the DLPFC with both positive and negative correlations to the subgenual.

Another possible reason for this shift toward a more positive correlation could be the nature of the neurodevelopment. Our results suggest that the activity patterns in DLPFC and the subgenual cingulate are more similar in adolescents and children than in adults. In other words, according to our findings, when the DLPFC is active in adolescents, it is more common to find the subgenual in a similar activity state in adolescents than in adults. It is not strange to find activity and connectivity disagreement between adult and pediatric populations considering the neurodevelopment differences between these two life stages. Adolescence is a period of drastic neuroplasticity and changes in neural structure and function, including areas involved in self-regulation such as the anterior cingulate cortex (ACC) (Lichenstein et al., 2016). This emphasizes the importance of optimizing the treatment for depression and other mental

disorders specifically in the population of interest. Future studies should evaluate the changes in subgenual correlation from childhood to adulthood.

One final explanation for these differences could be originated in the noise removal process. Variation in the data processing procedure can have a tremendous impact in the outcomes (see the

Global Signal Regression Debate section below). While our goal was to replicate the methods in Fox et al. (2012) as closely as possible, we had to make some personal decisions due to differences in the data set or the inability to find some very specific methodological information in Fox et al. (2012), Fox et al. (2005) or Van Dijk et al. (2010). This could have introduced some deviation from Fox et al. (2012) results.

The last item for discussion from our experiment 1 outcomes is the comparison with the control group. We obtained that individuals with MDD had a more positive DLPFC-Subgenual correlation for all seven targeting approaches, although the differences were not significant. These results do not seem to align with previous studies that show that adolescents with MDD or at familial risk of depression have a decreased functional connectivity between subgenual anterior cingulate cortex and cognitive control network (Cullen et al., 2009; Chai et al., 2016; Gaffrey et al., 2010). We have not been able to provide an educated guess of what could be causing this divergence. However, we must take into account that we did not find a significant difference between TRD and TDC groups. This prevent us from assuring with confidence whether there is an actual difference between the connectivity in youth with TRD and controls.

DLPFC-Subgenual Connectivity and Clinical Efficacy in Adolescents

Fox et al. (2012) ends up proposing an alternative targeting method based on the intrinsic networks of each individual (connectivity-based approach) in 2012. We attempted to investigate this association in experiment 2. As opposed to their results, we obtained that higher positive correlation between the individual sites of stimulation and the subgenual cingulate is associated with a decrease in the Ham-D score. This is not only contrary to Fox et al. (2012) results, but also to Weigand et al. (2018) and Cash al. (2019), who reported that the treatment response is higher when the anticorrelation is higher. To our knowledge, no studies in adolescents have studied this relationship. The initial positive-shifted DLPFC-Subgenual correlations (instead of anticorrelation) in the TRD group in our first experiment, could be strictly related to the differences in the association with clinical efficacy with the studies in adults. Furthermore, when we removed the outlier from the dataset (see **Figure 8**), the correlation with treatment response decreased from 0.39 to 0.20 and became nonsignificant. Even though this data point is not extreme and follows the trend, it may be largely driving the correlation. Coincidentally, a more recent study has pinpointed that the correlation with clinical efficacy in Fox et al. (2012) is also significantly dragged to the more negative end by an outlier (Jing et al., 2020). Regardless of this divergence, the results in experiment 2 seem consistent with the ones experiment 1, where the TRD group presents more positive correlations than the control group. We could think that the rTMS has caused a decrease in the positive correlation between the DLPFC and the

subgenual cingulate. Nevertheless, this should be corroborated in a longitudinal study where the DLPFC-Subgenual connectivity is calculated before and after treatment.

Fit to Networks in Depression

The most recent literature considers depression a network disorder where several interconnected brain structures can be dysregulated (Mayberg, 2007; Pitsillou et al., 2020). Among them, DLPFC and subgenual cingulate have received great attention because they appear consistently affected. Individuals with depression have distinct hypoactivity in the left DLPFC and hyperactivity in the subgenual cingulate (Dean and Keshavan, 2017; Pitsillou et al., 2020). Additionally, increase in activity in the DLPFC and decrease in activity in the subgenual cingulate is associated with an antidepressant effect (Drevets et al., 2008; Koenigs and Grafman, 2009). Looking at our results close enough, we can observe that in experiment 1, the correlations for TRD and TDC groups follow a very similar pattern whereas BA46, Rusjan, Paus and Fitzgerald have the lowest correlations, and Average 5, BA9 and EEGF3 have the highest ones. This is also consistent with figure 2 in Fox et al. (2012), even if the correlations in our results are shifted to more positive values. This means that specific sites within the DLPFC experience specific levels of correlation with the subgenual cingulate when compared with the other sites in the DLPFC. For instance, more posterior and medial regions in the DLPFC (such as the Average 5) express higher correlations than regions that the ones that are more anterior and lateral (such as BA46). From these results, we could say that DLPFC and subgenual cingulate are regions intrinsically related during resting-state, and thus, that the dysregulation of one of the regions could be caused by abnormalities in the other. Furthermore, this has a direct implication in the mechanism of rTMS in depression. If these two regions are intrinsically

connected in some way (whether positively, negatively or both), it would be logical to think that the stimulation of the DLPFC by TMS, which causes changes in activity of this region, could also trigger changes in activity in deep limbic regions that are also affected in depression, such as the subgenual cingulate. The use of the DLPFC-sgACC network to reduce the symptomatology of depression seems an appropriate method of targeting this condition as suggested in Jing et al. (2020).

Global Signal Regression Debate

There is a current debate as to whether global signal regression (GSR) should be included as a preprocessing step when studying networks in resting-state functional MRI scans. The goal of removing the whole-brain signal from the analysis is to discard effects of motion, respiration and cardiac rhythms in the overall bold signal (Li et al., 2019). The use of global signal regression has been associated with the appearance of robust negative correlations. This could be occurring because the negative correlations are only detected once the global artifacts are removed, but also this method itself could be shifting the correlations to the negative end due to a change in the correlation distribution (Fox et al., 2009; Chang and Glover, 2009). Li et al. (2019) shows that GSR is very effective in reducing artifacts due to motion and respiration in young adults. However, the decision as to use GSR is currently on the investigators' hands. In any case, it is suggested that researchers should not interpret the magnitude of the correlations when GSR is part of the data processing (Van Dijk et al., 2010). This is the reason why we must be very careful extracting conclusion from the interpretation of the correlation specific magnitudes from our experiments.

We have directly approached this debate by reporting the correlation between the DLPFC targets (experiment 1) and the subgenual cingulate before GSR was applied. The product of that is **Figure 7**. Whole-brain signal regression caused a decrease in the correlation values (**Figure 5**), including the shift of positive to negative correlations in several of the targeting methods for both TRD and TDC groups. We can conclude that at least, in our case, correlations between two regions of interest in resting-state fMRI are shifted to the negative end after whole-brain signal regression. Due to the evidence in the literature, we trust that this procedure successfully removed significant noise produced by physiological sources as well. However, it is unclear whether this process also shifted the correlations due to a mathematical redistribution of the data points. We believe future studies should employ different GSR methods to observe any changes among them and with non-regressed data.

Limitations

There are several limitations that could have had serious implications in our study. To begin with, we were unable to find some of the Fox et al. (2012) methodology details for data processing, among which the precise steps to remove global signal is the most relevant one. Considering the changes in correlation that global signal regression can create as discussed previously, we think that small differences in the GSR process or other steps to remove artifacts could have exacerbated the differences in the outcomes. Another limitation we encounter is the duration of the resting-state fMRI. Our scans had a length of 5 minutes. This is accepted in children (White et al., 2014). However, if we want to see an increase in both reliability and in-depth analysis without sacrificing safety, it is suggested to carry scans of ~13 minutes (Birn et

al., 2014). A third limitation has to do with adapting adult coordinates to the pediatric population. For this study we used the coordinates for seven different TMS targeting approaches that were performed in adults. That is, we were using adult coordinates in children and adolescent's brains. Considering that the head circumference keeps increasing until late adolescence (Kara et al., 2016), we might have placed our DLPFC ROIs in functionally different regions in the brain. This fact has most likely a significant impact in the subgenual correlation values. Nevertheless, the lack of rTMS practice in pediatric population leaves us very few data regarding different targeting methods for TMS in youth with MDD.

Future Work

In first place, an appropriate extension of this work would be to measure the changes in subgenual correlation before and after treatment in the experiment 2 sample. Additionally, since the results in experiment 1 and 2 are quite opposite to the literature, a replication of this study would be convenient. When attempting to do so, future work should try to minimize the limitations that emerged in the present study. First, fMRI scans should be acquired for approximately thirteen minutes as it is currently recommended. Additionally, more studies should quantify the effect of using different global signal regression methods when specifically looking at DLPFC-Subgenual correlations in a pediatric population. Alternatively, they could compare different techniques used for noise reduction. We believe that if the threshold for head motion correction, which we set at 0.5 mm, is considerably reduced at around 0.2 mm the data would appear cleaner for analysis (Byrge and Kennedy, 2018; Power et al., 2012).

On the other hand, we cannot disregard the positive correlation between the DLPFC-Subgenual connectivity and clinical efficacy that we found in our second experiment. This suggest that intrinsic connectivity patterns can be used to predict treatment response. Therefore, connectivity-based approach for rTMS targeting should be further investigated for depression treatment in adolescents. If replication studies confirm our findings in this population and demonstrate that there is an association between the DLPFC-Subgenual connectivity and the clinical efficacy, future clinical trials should implement rTMS using the connectivity-based approach. In this sense, our lab has a plan of attack to continue this line of research. We aim to corroborate the efficiency of the connectivity-based targeting approach in a larger sample. To address this, our lab will use data from the new Adolescent Depression and Other Psychiatric disorders TMS (ADAPT) clinic, in which adolescents with TRD will be divided into two groups based on the method used to determine. One of them will receive rTMS over the site of stimulation: connectivity-based approach andthe DLPFC associated with a higher treatment response. In the other group, the DLPFC will be targeted using the 5 centimetres rule respectively. Consequently, we will be able to compare the clinical efficacy between these two targeting strategies.

Conclusion

The current research project aimed to investigate the efficacy of the connectivity-based approach to determine the rTMS target in adolescents with TRD. We found that the connectivity between the DLPFC and subgenual cingulate in adolescents seems to differ from adults demonstrating the importance of doing mental health research specifically in pediatric samples.

Additionally, our results confirm that small differences in the location of the rTMS site within the left DLPFC can translate in significant differences in treatment response. Thus, defining an appropriate targeting method in this population is very relevant.

Addressing our specific aims, we found that only three out of the seven targeting approaches showed subgenual anticorrelation. This shift toward the positive end was higher than in the control group. Secondly, our outcomes showed that higher positive correlation is associated with a greater decrease in depression symptomatology. Nonetheless, the contrariety of our results to the literature and the novelty of this study makes it necessary to replicate the experiments performed while reducing some of the sources of error. In the end, we moved a step closer to our overall goal of improving the treatment options for such a debilitating disease in a very vulnerable population.

CHAPTER 5: SUPPLEMENTARY MATERIAL

DLPFC-Subgenual Correlation Steps

This section is used to sequentially present the steps followed to calculate the correlation between the seven targeting approaches DLPFC ROIs and the Subgenual Cingulate ROI at a subject level (first-level analysis). The description below includes parameters that were set as we worked through the optimization of each of the steps for an easier replication if needed. Although this refers specifically to experiment 1, experiment 2 followed the same procedure but with individual coordinates for one single DLPFC ROI (actual site of stimulation for rTMS).

1. Conversion of the images from DICOM to NIfTI using MRIcroGL.
2. ROIs spheres. We generated the subgenual cingulate ROI and the seven different DLPFC ROIs corresponding to the seven different targeting approaches using the coordinates defined in Fox et al. (2012). The voxels outside of the cortex were eliminated by using the binarized version of the left cortex Harvard-Oxford structural area thresholded at an intensity of 70. The DLPFC spherical ROIs for the targeting methods are depicted in **Figure 3.**
3. Sources of variance. From the Harvard-Oxford atlas available in FSL, we obtained the structural areas corresponding to the lateral ventricles (bilaterally) and the deep white matter (bilaterally), thresholded them at an intensity of 70 and binarized them. Similarly, we binarized the whole brain MNI standard image to use as a global signal. These three masks were later used in step 8.
4. Initial FSL steps. This includes brain extraction (BET) and brain reorientation for the structural and the fMRI images. The brain extraction of the anatomical image was

computed by robust brain center estimation because the input data contained a significant amount of non-brain matter. The fractional intensity threshold for brain extraction was set individually ranging from 0.10 to 0.80.

5. First-level preprocessing (FEAT). Following Fox et al. (2012) indications, the first 4 volumes were deleted, frequencies lower than 0.01 Hz were eliminated and spatial smoothing was set to 6 mm FWHM. The motion correction tool called MCFLIRT was applied. We also used slice timing correction, as our scans were collected interleaved.
6. Intensity scaling. The filtered image was transformed to a new image were the intensity values ranged from 0 to 1000.
7. Registration (FLIRT+FNIRT). After scaling, the functional data was registered to the MNI152 standard space via the anatomical image through linear (FLIRT) followed by non-linear (FNIRT) registration as suggested in the FNIRT user guide (Andersson, et al., 2010). The Rigid Body model (6 degrees of freedom) was used for linear registration.
8. Time series extraction (noise). By using the filtered functional image transformed to MNI space and the masks created in step 3, we extracted the average signal of the whole brain and the average signal within the voxels corresponding to the lateral ventricles and the deep white matter masks. The resulting files were used in step 11.
9. Motion parameters partition. In the preprocessing step, a file containing the six motion parameters computed by rigid body and rotation was generated. We divided the parameters into six different files to be used in step 11.
10. Head Position. We accounted for head position changes by calculating the FDs (in millimetres) for each participant. We also obtained a plot displaying the 146 FD values

of the same individual. Last, a confound matrix with the volumes lying above the 0.5 mm threshold (outliers) was generated as well and used in the next step.

11. Noise Removal. Linear regression was used to remove the nine sources of variance defined previously: 6 motion parameters, global signal, signal from the lateral ventricles and white matter signal. The first temporal derivative was included to exclude the time shifted versions of the nine variance regressors. Temporal filtering was also applied in the model as the data had been filtered too.
12. Mean Addition. The mean signal image was mathematically added to the residual image (clean data without noise) generated in the previous step to return to the original range of intensity.
13. Time series extraction (ROIs). Using the image as a result of the addition of the mean signal, we extracted the time series from each of the DLPFC ROIs and the subgenual cingulate ROI.
14. Pearson's r Correlation DLPFC-Subgenual. The connectivity between the DLPFC and subgenual cingulate was calculated by a Pearson's Correlation Coefficient test, including the p-values.

Table 4 below displays the steps in a table format including the input and output files for each of them.

Table 4. Input and Output Files Processing Steps

Summary of the subject-level image analysis steps followed to obtain the connectivity between the EEG F3 DLPFC ROI and the other brain regions for a given subject X. The input and output files for each step are included.

	Input(s) file(s)	**Output(s) file(s)**
DICOM to NIFTI *[MRIcroGL]*	Ax_FSPGR_BRAVO_08mm scans	X_anat.nii.gz
	fMRI_Resting_State scans	X _func.nii.gz
ROIs Masks Creation *[fslmaths]*	MNI152_T1_2mm_brain.nii.gz	Subgenualsphere_thr_masked.nii.gz
	MNI152_T1_2mm_brain.nii.gz	EEGF3sphere_thr_masked.nii.gz
Sources of Variance (Noise) Masks Creation *[fslmaths]*	MNI152_T1_2mm_brain.nii.gz	MNI152_T1_2mm_brain_mask.nii.gz
	Harvard-Oxford atlas	lateral_ventricles_mask.nii.gz
	Harvard-Oxford atlas	deep_white_matter_mask.nii.gz
Brain Extraction *[BET]* **and Reorientation** *[fslreorient2std]*	X _anat.nii.gz	X _anat_brain_reorient.nii.gz
	X _func.nii.gz	X _func_brain_reorient.nii.gz
First-Level Preprocessing [FEAT]	X _func_brain_reorient.nii.gz	filtered_func_data.nii.gz
0-1000 Intensity Scaling *[fslstats & fslmaths]*	filtered_func_data.nii.gz	filtered_func_data_scaled.nii.gz
Registration *[FLIRT + FNIRT]*	filtered_func_data_scaled.nii.gz	filtered_func_data_transformed.nii.gz
Noise Time Series Extraction *[fslmeants]*	filtered_func_data_transformed.nii.gz	MNI152_T1_2mm_brain _ts.txt
	filtered_func_data_transformed.nii.gz	lateral_ventricles _ts.txt
	filtered_func_data_transformed.nii.gz	deep_white_matter _ts.txt
Motion Parameters Partition	prefiltered_func_data_mcf.par	prefiltered_func_data_mcf.par1 prefiltered_func_data_mcf.par2

		prefiltered_func_data_mcf.par3 prefiltered_func_data_mcf.par4 prefiltered_func_data_mcf.par5 prefiltered_func_data_mcf.par6
Head Position *[FSL Motion Outliers]*	X _func_brain_reorient.nii.gz	motion_values.txt motion_values_plot.png motion_confound.txt
First-Level Statistics - Noise Regression + Volume Censoring *[FEAT]*	filtered_func_data_transformed.nii.gz	res4d.nii.gz
Mean Addition *[fslmaths]*	res4d.nii.gz mean_func.nii.gz	res4d+mean.nii.gz
ROIs Time Series Extraction *[fslmeants]*	res4d+mean.nii.gz	EEGF3 _ts.txt
	res4d+mean.nii.gz	Subgenual_ts.txt
Pearson's r Correlations DLPFC-Subgenual *[RStudio]*	EEGF3 _ts.txt Subgenual_ts.txt	r correlation value

Supplementary Figures

(A)

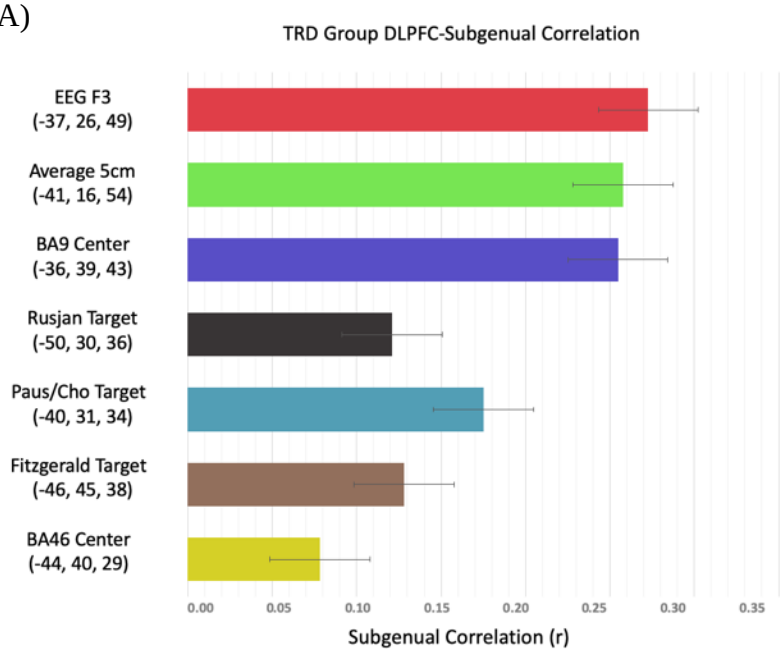

(B)

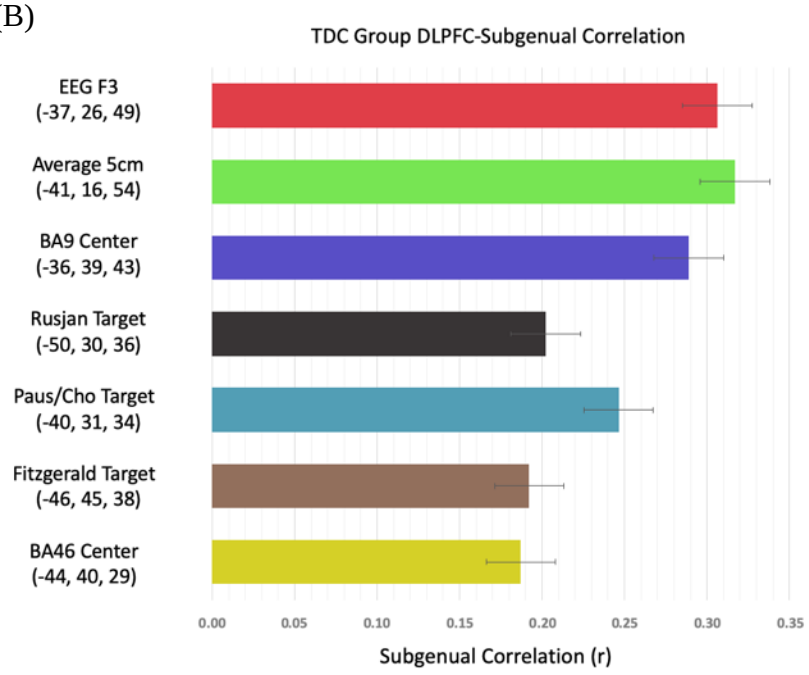

Figure 7. DLPFC-Subgenual Connectivity without Global Signal Regression

Variability of functional connectivity (expressed in mean Pearson's Correlation coefficient) between the subgenual cingulate and the seven different targeting approaches without global signal regression. Error bars reflect the standard error. S1A and S1B show the correlations for the TDR group and the TDC group, respectively.

(A)

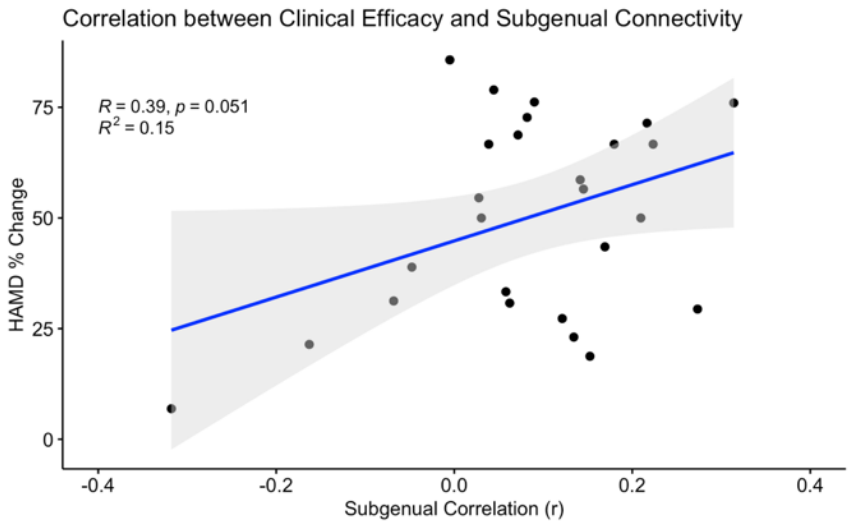

(B)

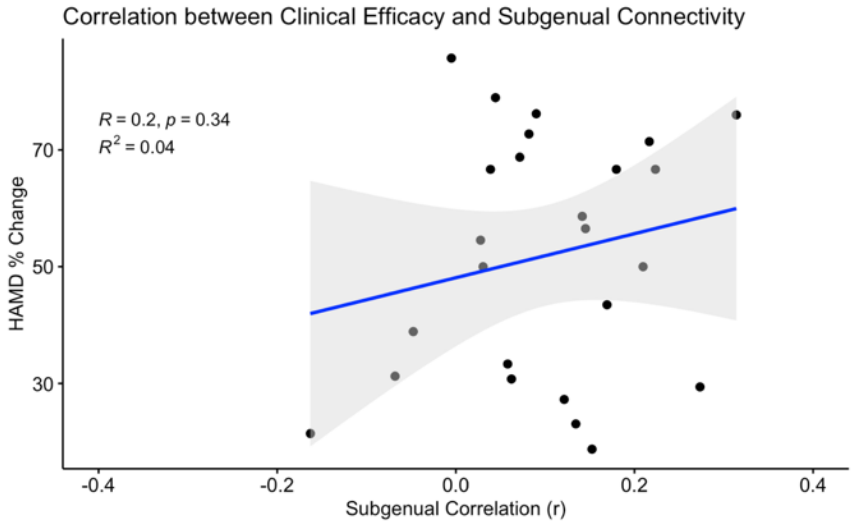

Figure 8. Outliers Testing for Experiment 2

Comparison of the correlation between the subgenual connectivity and clinical efficacy before (A) and after (B) the momentary deletion of the data point identified as an outlier. Grey area: 95% confidence interval for the linear fit.

CHAPTER 6: REFERENCES

American Psychiatric Association, 2013. Diagnostic and statistical manual of mental disorders: DSM-5. American Psychiatric Publishing, Inc.

Andersson, J.L.R., Jenkinson, M., Smith S., 2010. Non-linear registration, aka spatial normalisation.

Beck, A.T., Guth, D., Steer, R.A., Ball, R., 1997. Screening for major depression disorders in medical inpatients with the Beck Depression Inventory for Primary Care. Behaviour Research and Therapy 35, 785–791. https://doi.org/10.1016/S0005-7967(97)00025-9

Birn, R.M., Molloy, E.K., Patriat, R., Parker, T., Meier, T.B., Kirk, G.R., Nair, V.A., Meyerand, M.E., Prabhakaran, V., 2014. The effect of scan length on the reliability of resting-state fMRI connectivity estimates 20.

Byrge, L., Kennedy, D.P., 2018. Identifying and characterizing systematic temporally-lagged BOLD artifacts. NeuroImage 171, 376–392. https://doi.org/10.1016/j.neuroimage.2017.12.082

Borrione, L., Bellini, H., Boralli Razza, L., Avila, A.G., Baeken, C., Brem, A.-K., Busatto, G., Carvalho, A.F., Chekroud, A., Lotufo, P.A., da Grac, M., Martin, M., McClintock, S.M., Padberg, F., Passos, I.C., Salum, G.A., Vanderhasselt, M.-A., Fraguas, R., Benseñ or, I., Valiengo, L., Brunoni, A.R., 2019. Precision non-implantable neuromodulation therapies: a perspective for the depressed brain. Braz J Psychiatry 10. https://doi.org/10.1590/1516-4446

Brown, S., Rittenbach, K., Cheung, S., McKean, G., MacMaster, F.P., Clement, F., 2019. Current and Common Definitions of Treatment-Resistant Depression: Findings from a Systematic Review and Qualitative Interviews. Canadian Journal of Psychiatry. https://doi.org/10.1177/0706743719828965

Centers for Disease Control and Prevention, National Center for Health Statistics. Underlying Cause of Death 1999-2019 on CDC WONDER Online Database, released in 2020. Data are from the Multiple Cause of Death Files, 1999-2019, as compiled from data provided by the 57 vital statistics jurisdictions through the Vital Statistics Cooperative Program. Accessed at http://wonder.cdc.gov/ucd-icd10.html on Feb 1, 2021 2:17:49 PM

Chang, C., Glover, G.H., 2009. Effects of model-based physiological noise correction on default mode network anti-correlations and correlations. NeuroImage 47, 1448–1459. https://doi.org/10.1016/j.neuroimage.2009.05.012

Chai, X.J., Hirshfeld-Becker, D., Biederman, J., Uchida, M., Doehrmann, O., Leonard, J.A., Salvatore, J., Kenworthy, T., Brown, A., Kagan, E., de los Angeles, C., Gabrieli, J.D.E., Whitfield-Gabrieli, S., 2016. Altered Intrinsic Functional Brain Architecture in Children at Familial Risk of Major Depression. Biological Psychiatry 80, 849–858. https://doi.org/10.1016/j.biopsych.2015.12.003

Chen, G., Chen, G., Xie, C., Li, S.J., 2011. Negative functional connectivity and its dependence on the shortest path length of positive network in the resting-state human brain. Brain Connect 1(3), 195-206. https://doi.org/10.1089/brain.2011.0025.

Chen, L.C., Chen, Y.H., Bai, Y.M., Chen, T.J., Chen, M.H., Su, T.P., 2020. Antidepressant resistance in adolescents with major depressive disorder: A nationwide longitudinal study. Journal of Affective Disorders 262, 293–297. https://doi.org/10.1016/j.jad.2019.11.038

Chesebro, J., Armes, K., Peterson, K., 2019. Focus on pharmacotherapy for depression. Nursing 2019 49.

Cole, E.J., Stimpson, K.H., Bentzley, B.S., Gulser, M., Cherian, K., Tischler, C., Nejad, R., Pankow, H., Choi, E., Aaron, H., Espil, F.M., Pannu, J., Xiao, X., Duvio, D., Solvason, H.B., Hawkins, J., Guerra, A., Jo, B., Raj, K.S., Phillips, A.L., Barmak, F., Bishop, J.H., Coetzee, J.P., DeBattista, C., Keller, J., Schatzberg, A.F., Sudheimer, K.D., Williams, N.R., 2020. Stanford Accelerated Intelligent Neuromodulation Therapy for Treatment-Resistant Depression. AJP 177, 716–726. https://doi.org/10.1176/appi.ajp.2019.19070720

Croarkin, P.E., Elmaadawi, A.Z., Aaronson, S.T., Schrodt, G.R., Holbert, R.C., Verdoliva, S., Heart, K.L., Demitrack, M.A., Strawn, J.R., 2021. Left prefrontal transcranial magnetic stimulation for treatment-resistant depression in adolescents: a double-blind, randomized, sham-controlled trial. Neuropsychopharmacol. 46, 462–469. https://doi.org/10.1038/s41386-020-00829-y

Croarkin, P.E., MacMaster, F.P., 2019. Transcranial Magnetic Stimulation for Adolescent Depression. Child and Adolescent Psychiatric Clinics of North America. https://doi.org/10.1016/j.chc.2018.07.003

Croarkin, P.E., Nakonezny, P.A., Deng, Z.-D., Romanowicz, M., Voort, J.L.V., Camsari, D.D., Schak, K.M., Port, J.D., Lewis, C.P., 2018. High-frequency repetitive TMS for suicidal ideation in adolescents with depression. Journal of Affective Disorders 239, 282–290. https://doi.org/10.1016/j.jad.2018.06.048

Cullen, K.R., Gee, D.G., Klimes-Dougan, B., Gabbay, V., Hulvershorn, L., Mueller, B.A., Camchong, J., Bell, C.J., Houri, A., Kumra, S., Lim, K.O., Castellanos, F.X., Milham, M.P., 2009. A preliminary study of functional connectivity in comorbid adolescent depression. Neuroscience Letters 460, 227–231. https://doi.org/10.1016/j.neulet.2009.05.022

Dean, J., Keshavan, M., 2017. The neurobiology of depression: An integrated view. Asian Journal of Psychiatry. https://doi.org/10.1016/j.ajp.2017.01.025

Drevets, W.C., Savitz, J., Trimble, M., 2008. The Subgenual Anterior Cingulate Cortex in Mood Disorders. CNS spectr. 13, 663–681. https://doi.org/10.1017/S1092852900013754

Duda, P., Hajka, D., Wójcicka, O., Rakus, D., Gizak, A., 2020. GSK3β: A Master Player in Depressive Disorder Pathogenesis and Treatment Responsiveness. Cells 9, 727. https://doi.org/10.3390/cells9030727

Fitzgerald, P.B., Hoy, K., McQueen, S., Maller, J.J., Herring, S., Segrave, R., Bailey, M., Been, G., Kulkarni, J., Daskalakis, Z.J., 2009. A randomized trial of rTMS targeted with MRI based neuro-navigation in treatment-resistant depression. Neuropsychopharmacology 34, 1255–1262. https://doi.org/10.1038/npp.2008.233

Fox, M.D., Buckner, R.L., White, M.P., Greicius, M.D., Pascual-Leone, A., 2012. Efficacy of transcranial magnetic stimulation targets for depression is related to intrinsic functional connectivity with the subgenual cingulate. Biological Psychiatry 72, 595–603. https://doi.org/10.1016/j.biopsych.2012.04.028

Fox, M.D., Zhang, D., Snyder, A.Z., Raichle, M.E., 2009. The Global Signal and Observed Anticorrelated Resting State Brain Networks. Journal of Neurophysiology 101, 3270–3283. https://doi.org/10.1152/jn.90777.2008

Fox, M.D., Raichle, M.E., 2007. Spontaneous fluctuations in brain activity observed with functional magnetic resonance imaging. Nat Rev Neurosci 8, 700–711. https://doi.org/10.1038/nrn2201

Fox, M.D., Snyder, A.Z., Vincent, J.L., Corbetta, M., Raichle, M.E., n.d., 2005. The human brain is intrinsically organized into dynamic, anticorrelated functional networks 6.

Fregni, F., Marcolin MA, Myczkowski M, Amiaz R, Hasey G, Rumi DO, et al. (2006): Predictors of antidepressant response in clinical trials of transcranial magnetic stimulation. Int J Neuropsychopharmacol. 9:641-654.

Frieden, T.R., Harold Jaffe, D.W., Cardo, D.M., Moolenaar, R.L., Leahy, M.A., Martinroe, J.C., Spriggs, S.R., Starr, T.M., Doan, Q.M., King, P.H., Roper, W.L., Hill, C., Matthew Boulton, C.L., Arbor, A., Virginia Caine, M.A., Barbara Ellis, I.A., Jonathan Fielding, G.E., Jones, T.F., Rima Khabbaz, T.F., Dennis Maki, G.G., Patricia Quinlisk, W., Moines, D., Patrick Remington, I.L., John Rullan, W. v, Juan, S., William Schaffner, P.,

2013. Mental Health Surveillance Among Children — United States, 2005–2011, MMWR.

Gaffrey, M.S., Luby, J.L., Repovš, G., Belden, A.C., Botteron, K.N., Luking, K.R., Barch, D.M., 2010. Subgenual cingulate connectivity in children with a history of preschool-depression. NeuroReport 21, 1182–1188. https://doi.org/10.1097/WNR.0b013e32834127eb

Garvey, M.A., 2005. Chapter 30 - Transcranial Magnetic Stimulation Studies in Children, in: Hallett, M., Chokroverty, S. (Eds.), Magnetic Stimulation in Clinical Neurophysiology (Second Edition). Butterworth-Heinemann, Philadelphia, pp. 429–437. https://doi.org/https://doi.org/10.1016/B978-0-7506-7373-0.50033-X

George, M.S., Lisanby, S.H., Avery, D., Mcdonald, W.M., Durkalski, V., Pavlicova, M., Anderson, ; Berry, Nahas, Z., Bulow, P., Zarkowski, P., Holtzheimer, P.E., Schwartz, T., Sackeim, H.A., 2010. Daily Left Prefrontal Transcranial Magnetic Stimulation Therapy for Major Depressive Disorder: A Sham-Controlled Randomized Trial, GEN PSYCHIATRY.

Gould, M.S., King, R., Greenwald, S., Fisher, P., Schwab-Stone, M., Kramer, R., Flisher, A.J., Goodman, S., Canino, G., Shaffer, D., 1998. Psychopathology associated with suicidal ideation and attempts among children and adolescents. Journal of the American Academy of Child and Adolescent Psychiatry 37, 915–923. https://doi.org/10.1097/00004583-199809000-00011

Greicius, M.D., Flores, B.H., Menon, V., Glover, G.H., Solvason, H.B., Kenna, H., Reiss, A.L., Schatzberg, A.F., 2007. Resting-State Functional Connectivity in Major Depression: Abnormally Increased Contributions from Subgenual Cingulate Cortex and Thalamus. Biological Psychiatry 62, 429–437. https://doi.org/10.1016/j.biopsych.2006.09.020

Hamilton, M., 1960. A rating scale for depression. J Neurol Neurosurg Psychiatry 23, 56-62.

Hamilton, M., 1967. Development of a Rating Scale for Primary Depressive Illness. British Journal of Social and Clinical Psychology 6, 278–296. https://doi.org/10.1111/j.2044-8260.1967.tb00530.x

Hamilton, M., 1959. The assessment of anxiety states by rating. British Journal of Medical Psychology 32, 50–55. https://doi.org/10.1111/j.2044-8341.1959.tb00467.x

Herbsman, T., Avery, D., Ramsey, D., Holtzheimer, P., Wadjik, C., Hardaway, F., Haynor, D., George, M.S., Nahas, Z., 2009. More Lateral and Anterior Prefrontal Coil Location Is Associated with Better Repetitive Transcranial Magnetic Stimulation Antidepressant Response. Biological Psychiatry 66, 509–515. https://doi.org/10.1016/j.biopsych.2009.04.034

Herwig, U., Lampe, Y., Juengling, F.D., Wunderlich, A., Walter, H., Spitzer, M., Schönfeldt-Lecuona, C., 2003. Add-on rTMS for treatment of depression: A pilot study using stereotaxic coil-navigation according to PET data. Journal of Psychiatric Research 37, 267–275. https://doi.org/10.1016/S0022-3956(03)00042-6

Herwig, U., Padberg, F., Unger, J., Spitzer, M., Schönfeldt-Lecuona, C., 2001. TECHNIQUES AND METHODS Transcranial Magnetic Stimulation in Therapy Studies: Examination of the Reliability of "Standard" Coil Positioning by Neuronavigation.

Hirshfeld-Becker, D.R., Gabrieli, J.D.E., Shapero, B.G., Biederman, J., Whitfield-Gabrieli, S., Chai, X.J., 2019. Intrinsic Functional Brain Connectivity Predicts Onset of Major Depression Disorder in Adolescence: A Pilot Study. Brain Connectivity 9, 388–398. https://doi.org/10.1089/brain.2018.0646

Jing, Y., Zhao, N., Deng, X., Feng, Z., Huang, G., Meng, M., Zang, Y., Wang, J., 2020. Pregenual or subgenual anterior cingulate cortex as potential effective region for brain stimulation of depression. Brain Behav 10. https://doi.org/10.1002/brb3.1591

Johnston, J.A.Y., Wang, F., Liu, Jie, Blond, B.N., Wallace, A., Liu, Jiacheng, Spencer, L., Cox Lippard, E.T., Purves, K.L., Landeros-Weisenberger, A., Hermes, E., Pittman, B., Zhang, S., King, R., Martin, A., Oquendo, M.A., Blumberg, H.P., 2017. Multimodal Neuroimaging of Frontolimbic Structure and Function Associated With Suicide Attempts in Adolescents and Young Adults With Bipolar Disorder. AJP 174, 667–675. https://doi.org/10.1176/appi.ajp.2016.15050652

Kara, B., Etiler, N., Aydogan Uncuoglu, A., Maras Genc, H., Ulak Gumuslu, E., Gokcay, G., Furman, A., 2016. Head Circumference Charts for Turkish Children Aged Five to Eighteen Years. Arch Neuropsychiatr 53, 52–59. https://doi.org/10.5152/npa.2015.10202

Kaufman, J., Birmaher, B., Brent, D., Rao, U., Flynn, C., Moreci, P., Williamson, D., Ryan, N., 1997. Schedule for affective disorders and schizophrenia for school-age children-present

and lifetime version (K-SADS-PL): Initial reliability and validity data. Journal of the American Academy of Child and Adolescent Psychiatry 36, 980–988. https://doi.org/10.1097/00004583-199707000-00021

Kessler, R.C., Avenevoli, S., Ries Merikangas, K., 2001. Mood disorders in children and adolescents: an epidemiologic perspective. Biological Psychiatry 49, 1002–1014. https://doi.org/10.1016/S0006-3223(01)01129-5

Kirton, A., deVeber, G., Gunraj, C., Chen, R., 2010. Cortical excitability and interhemispheric inhibition after subcortical pediatric stroke: Plastic organization and effects of rTMS. Clinical Neurophysiology 121, 1922–1929. https://doi.org/10.1016/j.clinph.2010.04.021

Koenigs, M., Grafman, J., 2009. The functional neuroanatomy of depression: Distinct roles for ventromedial and dorsolateral prefrontal cortex. Behavioural Brain Research 201, 239–243. https://doi.org/10.1016/j.bbr.2009.03.004

Kuehner, C., 2017. Why is depression more common among women than among men? The Lancet Psychiatry. https://doi.org/10.1016/S2215-0366(16)30263-2

Lefaucheur, J.P., Aleman, A., Baeken, C., Benninger, D.H., Brunelin, J., di Lazzaro, V., Filipović, S.R., Grefkes, C., Hasan, A., Hummel, F.C., Jääskeläinen, S.K., Langguth, B., Leocani, L., Londero, A., Nardone, R., Nguyen, J.P., Nyffeler, T., Oliveira-Maia, A.J., Oliviero, A., Padberg, F., Palm, U., Paulus, W., Poulet, E., Quartarone, A., Rachid, F., Rektorová, I., Rossi, S., Sahlsten, H., Schecklmann, M., Szekely, D., Ziemann, U., 2020. Evidence-based guidelines on the therapeutic use of repetitive transcranial magnetic

stimulation (rTMS): An update (2014–2018). Clinical Neurophysiology. https://doi.org/10.1016/j.clinph.2019.11.002

Leggett LE, Coward S, Soril LJJ, Mackean G, Lorenzetti D, Clement F (2014): Repetitive Transcranial Magnetic Stimulation for Treatment Resistant Depression: A Health Technology Assessment. University of Calgary.

Li, J., Kong, R., Liégeois, R., Orban, C., Tan, Y., Sun, N., Holmes, A.J., Sabuncu, M.R., Ge, T., Yeo, B.T.T., 2019. Global signal regression strengthens association between resting-state functional connectivity and behavior. NeuroImage 196, 126–141. https://doi.org/10.1016/j.neuroimage.2019.04.016

Lichenstein, S.D., Verstynen, T., Forbes, E.E., 2016. Adolescent brain development and depression: A case for the importance of connectivity of the anterior cingulate cortex. Neuroscience & Biobehavioral Reviews 70, 271–287. https://doi.org/10.1016/j.neubiorev.2016.07.024

Lima-Ojeda, J.M., Rupprecht, R., Baghai, T.C., 2018. Neurobiology of depression: A neurodevelopmental approach. World Journal of Biological Psychiatry. https://doi.org/10.1080/15622975.2017.1289240

Lipari, R.N., Park-Lee, E., 2019. Key Substance Use and Mental Health Indicators in the United States: Results from the 2018 National Survey on Drug Use and Health.

Liston, C., Chen, A.C., Zebley, B.D., Drysdale, A.T., Gordon, R., Leuchter, B., Voss, H.U., Casey, B.J., Etkin, A., Dubin, M.J., 2014. Default Mode Network Mechanisms of

Transcranial Magnetic Stimulation in Depression. Biological Psychiatry 76, 517–526. https://doi.org/10.1016/j.biopsych.2014.01.023

MacMaster, F.P., Croarkin, P.E., Wilkes, T.C., McLellan, Q., Langevin, L.M., Jaworska, N., Swansburg, R.M., Jasaui, Y., Zewdie, E., Ciechanski, P., Kirton, A., 2019. Repetitive transcranial magnetic stimulation in youth with treatment resistant major depression. Frontiers in Psychiatry 10. https://doi.org/10.3389/fpsyt.2019.00170

MacMaster, F.P., Russell, A., Mirza, Y., Keshavan, M.S., Taormina, S.P., Bhandari, R., Boyd, C., Lynch, M., Rose, M., Ivey, J., Moore, G.J., Rosenberg, D.R., 2006. Pituitary Volume in Treatment-Naïve Pediatric Major Depressive Disorder. Biological Psychiatry 60, 862–866. https://doi.org/10.1016/j.biopsych.2006.04.013

MacQueen, G.M., Frey, B.N., Ismail, Z., Jaworska, N., Steiner, M., Lieshout, R.J.V., Kennedy, S.H., Lam, R.W., Milev, R. v., Parikh, S. v., Ravindran, A. v., 2016. Canadian Network for Mood and Anxiety Treatments (CANMAT) 2016 clinical guidelines for the management of adults with major depressive disorder: Section 6. Special populations: Youth, women, and the elderly. Canadian Journal of Psychiatry. https://doi.org/10.1177/0706743716659276

Magavi, L.R., Reti, I.M., Vasa, R.A., 2017. A review of repetitive transcranial magnetic stimulation for adolescents with treatment-resistant depression. International Review of Psychiatry. https://doi.org/10.1080/09540261.2017.1300574

Malhi, G.S., Mann, J.J., 2018. Depression. The Lancet. https://doi.org/10.1016/S0140-6736(18)31948-2

Margulies, D.S., Kelly, A.M.C., Uddin, L.Q., Biswal, B.B., Castellanos, F.X., Milham, M.P., 2007. Mapping the functional connectivity of anterior cingulate cortex. NeuroImage 37, 579–588. https://doi.org/10.1016/j.neuroimage.2007.05.019

Mayberg, H.S., 2007. Defining the Neural Circuitry of Depression: Toward a New Nosology With Therapeutic Implications. Biological Psychiatry 61, 729–730. https://doi.org/10.1016/j.biopsych.2007.01.013

McClintock, S.M., Reti, I.M., Carpenter, L.L., McDonald, W.M., Dubin, M., Taylor, S.F., Cook, I.A., O'Reardon, J., Husain, M.M., Wall, C., Krystal, A.D., Sampson, S.M., Morales, O., Nelson, B.G., Latoussakis, V., George, M.S., Lisanby, S.H., 2018. Consensus recommendations for the clinical application of repetitive transcranial magnetic stimulation (rTMS) in the treatment of depression. Journal of Clinical Psychiatry. https://doi.org/10.4088/JCP.16cs10905

Milev, R. V., Giacobbe, P., Kennedy, S. H., Blumberger, D. M., Daskalakis, Z. J., Downar, J., et al. (2016). Canadian Network for Mood and Anxiety Treatments (CANMAT) 2016 Clinical Guidelines for the Management of Adults with Major Depressive Disorder: Section 4. Neurostimulation Treatments. The Canadian Journal of Psychiatry, 61(9), 561–575. https://doi.org/10.1177/0706743716660033

Mullen, S., 2018. Major depressive disorder in children and adolescents. Mental Health Clinician 8, 275–283. https://doi.org/10.9740/mhc.2018.11.275

Narang, P., Madigan, K., Sarai, S., Lippmann, S., 2019. Is Transcranial Magnetic Stimulation Appropriate For Treating Adolescents with Depression? Innovations in Clinical Neuroscience 6, 30–35.

neuroCare Group, 2017. Combined rTMS and Psychotherapy an effective treatment for Depression - neuroCare Group [WWW Document]. URL https://www.neurocaregroup.com/press-details/combined-rtms-and-psychotherapy-an-effective-treatment-for-depression.html (accessed 4.25.20).

O'Reardon, J.P., Solvason, H.B., Janicak, P.G., Sampson, S., Isenberg, K.E., Nahas, Z., McDonald, W.M., Avery, D., Fitzgerald, P.B., Loo, C., Demitrack, M.A., George, M.S., Sackeim, H.A., 2007. Efficacy and Safety of Transcranial Magnetic Stimulation in the Acute Treatment of Major Depression: A Multisite Randomized Controlled Trial. Biological Psychiatry 62, 1208–1216. https://doi.org/10.1016/j.biopsych.2007.01.018

Park, C., Rosenblat, J.D., Lee, Y., Pan, Z., Cao, B., Iacobucci, M., McIntyre, R.S., 2019. The neural systems of emotion regulation and abnormalities in major depressive disorder. Behavioural Brain Research. https://doi.org/10.1016/j.bbr.2019.04.002

Park, R., Goodyer, M., 2000. Clinical guidelines for depressive disorders in childhood and adolescence. European Child & Adolescent Psychiatry 9, 147–161.

Park, S.-C., Kim, J.-M., Jun, T.-Y., Lee, M.-S., Kim, J.-B., Yim, H.-W., & Park, Y. C. (2017). How many different symptom combinations fulfil the diagnostic criteria for major depressive disorder? Results from the CRESCEND study. Nordic Journal of Psychiatry, 71(3), 217–222. https://doi.org/10.1080/08039488.2016.1265584

Parente, F., Colosimo, A., 2018. Anticorrelations between Active Brain Regions: An Agent-Based Model Simulation Study. Neural Plasticity 2018, 1–11. https://doi.org/10.1155/2018/6815040

Pitsillou, E., Bresnehan, S.M., Kagarakis, E.A., Wijoyo, S.J., Liang, J., Hung, A., Karagiannis, T.C., 2020. The cellular and molecular basis of major depressive disorder: towards a unified model for understanding clinical depression. Molecular Biology Reports. https://doi.org/10.1007/s11033-019-05129-3

Pizzagalli, D.A., Holmes, A.J., Daniel Dillon, A.G., Goetz, E.L., Jeffrey Birk, B.L., Ryan Bogdan, B., Darin Dougherty, A.D., Iosifescu, D. v, Rauch, S.L., Fava, M., 2009. Article Reduced Caudate and Nucleus Accumbens Response to Rewards in Unmedicated Individuals With Major Depressive Disorder, Am J Psychiatry.

Power, J.D., Barnes, K.A., Snyder, A.Z., Schlaggar, B.L., Petersen, S.E., 2012. Spurious but systematic correlations in functional connectivity MRI networks arise from subject motion. NeuroImage 59, 2142–2154. https://doi.org/10.1016/j.neuroimage.2011.10.018

Poznanski, E., Freeman, L., Mokros, H., 1985. Children's depression rating scale-revised. Psychopharmacol Rev 21, 979–89.

Rajkowska, G., Goldman-Rakic, P.S., 1995. Cytoarchitectonic Definition of Prefrontal Areas in the Normal Human Cortex: II. Variability in Locations of Areas 9 and 46 and Relationship to the Talairach Coordinate System. Cerebral Cortex 5, 323–337.

Rush, A.J., Kraemer, H.C., Sackeim, H.A., Fava, M., Trivedi, M.H., Frank, E., Ninan, P.T., Thase, M.E., Gelenberg, A.J., Kupfer, D.J., Regier, D.A., Rosenbaum, J.F., Ray, O.,

Schatzberg, A.F., 2006. Report by the ACNP Task Force on response and remission in major depressive disorder. Neuropsychopharmacology 31, 1841–1853. https://doi.org/10.1038/sj.npp.1301131

Rusjan, P.M., Barr, M.S., Farzan, F., Arenovich, T., Maller, J.J., Fitzgerald, P.B., Daskalakis, Z.J., 2010. Optimal transcranial magnetic stimulation coil placement for targeting the dorsolateral prefrontal cortex using novel magnetic resonance image-guided neuronavigation. Human Brain Mapping 31, 1643–1652. https://doi.org/10.1002/hbm.20964

Sanches, M., Caetano, S., Nicoletti, M., Monkul, E.S., Chen, H.H., Hatch, J.P., Yeh, P.H., Mullis, R.L., Keshavan, M.S., Rajowska, G., Soares, J.C., 2009. An MRI-based approach for the measurement of the dorsolateral prefrontal cortex in humans. Psychiatry Research - Neuroimaging 173, 150–154. https://doi.org/10.1016/j.pscychresns.2009.02.007

Scharnowski, F., Nicholson, A.A., Pichon, S., Rosa, M.J., Rey, G., Eickhoff, S.B., Van De Ville, D., Vuilleumier, P., Koush, Y., 2020. The role of the subgenual anterior cingulate cortex in dorsomedial prefrontal–amygdala neural circuitry during positive-social emotion regulation. Hum Brain Mapp 41, 3100–3118. https://doi.org/10.1002/hbm.25001

Sheline, Y.I., 2003. Neuroimaging studies of mood disorder effects on the brain. Biological Psychiatry. https://doi.org/10.1016/S0006-3223(03)00347-0

Smith, D.F., Jakobsen, S., 2013. Molecular neurobiology of depression: PET findings on the elusive correlation with symptom severity. Frontiers in Psychiatry. https://doi.org/10.3389/fpsyt.2013.00008

Sokhadze, E.M., Lamina, E. v., Casanova, E.L., Kelly, D.P., Opris, I., Tasman, A., Casanova, M.F., 2018. Exploratory study of rTMS neuromodulation effects on electrocortical functional measures of performance in an oddball test and behavioral symptoms in autism. Frontiers in Systems Neuroscience 12. https://doi.org/10.3389/fnsys.2018.00020

Thapar, A., Collishaw, S., Pine, D.S., Thapar, A.K., 2012. Seminar Child & Adolescent Psychiatry Section, Department of Psychological Medicine and Neurology (Prof A Thapar FRCPsych, S Collishaw DPhil, A K Thapar Depression in adolescence. The Lancet 379, 1056–1067. https://doi.org/10.1016/S0140

Tymofiyeva, O., Zhou, V.X., Lee, C.-M., Xu, D., Hess, C.P., Yang, T.T., 2020. MRI Insights Into Adolescent Neurocircuitry—A Vision for the Future. Front. Hum. Neurosci. 14, 237. https://doi.org/10.3389/fnhum.2020.00237

Van Dijk, K.R.A., Hedden, T., Venkataraman, A., Evans, K.C., Lazar, S.W., Buckner, R.L., 2010. Intrinsic Functional Connectivity As a Tool For Human Connectomics: Theory, Properties, and Optimization. Journal of Neurophysiology 103, 297–321. https://doi.org/10.1152/jn.00783.2009

Voineskos, D., Daskalakis, Z.J., Blumberger, D.M., 2020. Management of treatment-resistant depression: Challenges and strategies. Neuropsychiatric Disease and Treatment. https://doi.org/10.2147/NDT.S198774

White, T., Muetzel, R., Schmidt, M., Langeslag, S.J.E., Jaddoe, V., Hofman, A., Calhoun, V.D., Verhulst, F.C., Tiemeier, H., n.d. Time of Acquisition and Network Stability in Pediatric Resting-State Functional Magnetic Resonance Imaging 11.

Zewdie, E., Ciechanski, P., Kuo, H.C., Giuffre, A., Kahl, C., King, R., Cole, L., Godfrey, H., Seeger, T., Swansburg, R., Damji, O., Rajapakse, T., Hodge, J., Nelson, S., Selby, B., Gan, L., Jadavji, Z., Larson, J.R., MacMaster, F., Yang, J.F., Barlow, K., Gorassini, M., Brunton, K., Kirton, A., 2020. Safety and tolerability of transcranial magnetic and direct current stimulation in children: Prospective single center evidence from 3.5 million stimulations. Brain Stimulation 13, 565–575. https://doi.org/10.1016/j.brs.2019.12.025

Zimmerman, M., Ellison, W., Young, D., Chelminski, I., & Dalrymple, K. (2015). How many different ways do patients meet the diagnostic criteria for major depressive disorder? Comprehensive Psychiatry, 56, 29–34. https://doi.org/10.1016/j.comppsych.2014.09.007